Induction of Cross-Priming of Naive CD8$^+$ T Lymphocytes by Recombinant Bacillus Calmette-Guérin That Secretes Heat Shock Protein 70-Major Membrane Protein-II Fusion Protein[1]

Tetsu Mukai, Yumi Maeda, Toshiki Tamura, Masanori Matsuoka, Yumiko Tsukamoto, and Masahiko Makino[2]

Because *Mycobacterium bovis* bacillus Calmette-Guérin (BCG) unconvincingly activates human naive CD8$^+$ T cells, a rBCG (BCG-70M) that secretes a fusion protein comprising BCG-derived heat shock protein (HSP)70 and *Mycobacterium leprae*-derived major membrane protein (MMP)-II, one of the immunodominant Ags of *M. leprae*, was newly constructed to potentiate the ability of activating naive CD8$^+$ T cells through dendritic cells (DC). BCG-70M secreted HSP70-MMP-II fusion protein in vitro, which stimulated DC to produce IL-12p70 through TLR2. BCG-70M-infected DC activated not only memory and naive CD8$^+$ T cells, but also CD4$^+$ T cells of both types to produce IFN-γ. The activation of these naive T cells by BCG-70M was dependent on the MHC and CD86 molecules on BCG-70M-infected DC, and was significantly inhibited by pretreatment of DC with chloroquine. Both brefeldin A and lactacystin significantly inhibited the activation of naive CD8$^+$ T cells by BCG-70M through DC. Thus, the CD8$^+$ T cell activation may be induced by cross-presentation of Ags through a TAP- and proteosome-dependent cytosolic pathway. When naive CD8$^+$ T cells were stimulated by BCG-70M-infected DC in the presence of naive CD4$^+$ T cells, CD62L^{low}CD8$^+$ T cells and perforin-producing CD8$^+$ T cells were efficiently produced. MMP-II-reactive CD4$^+$ and CD8$^+$ memory T cells were efficiently produced in C57BL/6 mice by infection with BCG-70M. These results indicate that BCG-70M activated DC, CD4$^+$ T cells, and CD8$^+$ T cells, and the combination of HSP70 and MMP-II may be useful for inducing better T cell activation. *The Journal of Immunology*, 2009, 183: 6561–6568.

Leprosy is a chronic infectious disease induced by an intracellular infection with *Mycobacterium leprae* (1, 2). Host defense against *M. leprae* is chiefly conducted by adaptive immunity in which both IFN-γ-producing type 1 CD4$^+$ T cells and CD8$^+$ T cells play an important role, and the activation of these T cells inhibits the spread of *M. leprae* (3–5). The activation is induced by bacilli-loaded dendritic cells (DC),[3] which display one or more antigenic determinants of *M. leprae*. Previously, we identified major membrane protein (MMP)-II (gene name, bfrA or ML2038) as one of the immunodominant Ag of *M. leprae* (6). MMP-II activates dendritic cells (DC) by activating the NF-κB pathway as a consequence of TLR2's ligation, and DC pulsed with a rMMP-II protein activate both naive and memory-type CD4$^+$ and CD8$^+$ T cells to produce IFN-γ in an Ag-specific manner (6, 7). In the lesions of patients with paucibacillary leprosy, representative of clinical leprosy on one pole, the involvement of CD1a$^+$ DC and presence of substantially activated T cells have been observed (8, 9). Furthermore, MMP-II is thought to be recognized by both T cell subsets in *M. leprae*-infected individuals, including patients with paucibacillary leprosy (7). Therefore, MMP-II is considered to play essential roles in the induction of host defense activity against *M. leprae*. Also, we reported that T cells from lepromatous leprosy, representative of clinical leprosy on another pole, can be activated to produce IFN-γ when stimulated with MMP-II-pulsed autologous DC (7), although it is known that the T cells of lepromatous leprosy patients are usually unresponsive to *M. leprae*-derived Ags (2).

Mycobacterium bovis bacillus Calmette-Guérin (BCG) is the sole available vaccine against leprosy, and several reports have evaluated its efficacy. In some countries and endemic areas, BCG has effectively inhibited the development of leprosy, whereas in others, its efficacy is reported to be quite limited (10–12). These observations indicate that questions remain regarding the reliability of BCG as a vaccine, and, in fact, Setia et al. (13) elucidated the overall efficacy of BCG to be only 26% through meta-analyses of several studies and observations. Based on these findings, we previously produced a rBCG that secretes MMP-II intracytosolically (BCG-SM) (14). As expected, BCG-SM activated both naive CD4$^+$ and CD8$^+$ T cells (14) and inhibited *M. leprae* from multiplying to some extent, but not completely, in the footpads of C57BL/6 mice (Y. M., T. T., M. Mat., and M. Mak.; unpublished observations). It is known that the parental BCG activates chiefly CD4$^+$ T cells, and less efficiently activates naive CD8$^+$ T cells (15). That BCG-SM activated naive T cells of both subsets and, consequently, partially inhibited the multiplication of *M. leprae*,

Department of Mycobacteriology, Leprosy Research Center, National Institute of Infectious Diseases, Tokyo, Japan

Received for publication November 18, 2008. Accepted for publication September 12, 2009.

The costs of publication of this article were defrayed in part by the payment of page charges. This article must therefore be hereby marked *advertisement* in accordance with 18 U.S.C. Section 1734 solely to indicate this fact.

[1] This work was supported in part by a Grant-in-Aid for Research on Emerging and Re-emerging Infectious Diseases from the Ministry of Health, Labour, and Welfare of Japan.

[2] Address correspondence and reprint requests to Dr. Masahiko Makino, Department of Mycobacteriology, Leprosy Research Center, National Institute of Infectious Diseases, 4-2-1 Aobacho, Higashimurayama, Tokyo 189-0002, Japan. E-mail address: mmaki@nih.go.jp

[3] Abbreviations used in this paper: DC, dendritic cell; BCC, *Mycobacterium bovis* bacillus Calmette-Guérin-derived cytosolic protein; BCG, *Mycobacterium bovis* bacillus Calmette-Guérin; BCG-SM, rBCG that secretes major membrane protein-II; HSP, heat shock protein; MMP, major membrane protein; MOI, multiplicity of infection.

www.jimmunol.org/cgi/doi/10.4049/jimmunol.0803857

indicated that the secretion of an immunodominant Ag of *M. leprae* in phagosomes of APCs of host is a useful way to inhibit the growth of *M. leprae* through the activation of T cells by delivering the antigenic determinants on APCs. This point was also revealed in other intracellular infection systems such as *Mycobacterium tuberculosis*, in which the secretion of Ag85 complex, one of the immunogenic molecules of *M. tuberculosis*, from vaccinated BCG was revealed to be effective in inhibiting the replication of *M. tuberculosis* challenged subsequently (16). Although the mechanisms involved have not been fully clarified, the activation of $CD8^+$ T cells seems to be induced by Ag85 protein secreted from BCG (16).

In general, the most efficient immunological means of activating naive $CD8^+$ T cells using mycobacteria, including BCG, is to upregulate the activity of DC to cross-present mycobacteria-derived Ags to the $CD8^+$ T cells. In this respect, an active inducer of cross-presenting activity in APCs is heat shock protein (HSP)70 (17, 18). HSP70 may be closely associated with host defenses against intracellular pathogens such as mycobacteria (19, 20).

In this study, in the search for another tool capable of stimulating naive $CD8^+$ T cells efficiently, we newly constructed a rBCG having an extrachromosomal BCG-derived HSP70 gene linked to the gene encoding MMP-II of *M. leprae* (BCG-70M), and evaluated its immunostimulatory activities. The BCG-70M secreted the HSP70-MMP-II fusion protein in vitro, and DC infected with BCG-70M more efficiently activated not only naive $CD8^+$ T cells by cross-presentation, but also naive $CD4^+$ T cells. Furthermore, BCG-70M produced memory T cells, of both $CD4^+$ and $CD8^+$ subsets in mice, capable of responding to MMP-II.

Materials and Methods

Preparation of cells and Ags

Peripheral blood was obtained from healthy purified protein derivative-positive individuals under informed consent using a double-blind system. In Japan, a BCG vaccination is compulsory for children (0~4 years old). PBMCs were isolated using Ficoll-Paque PLUS (Pharmacia) and cryopreserved in liquid nitrogen until used, as described previously (21). For the preparation of peripheral monocytes, $CD3^+$ T cells were removed from either freshly isolated heparinized blood, or cryopreserved PBMCs using immunomagnetic beads coated with anti-CD3 mAb (Dynabeads 450; Dynal Biotech). The $CD3^-$ PBMC fraction was plated on collagen-coated plates, and the nonplastic-adherent cells were removed by extensive washing. The remaining adherent cells were used as monocytes (22). Monocyte-derived DC were differentiated, as described previously (21, 23). Briefly, monocytes were cultured in the presence of 50 ng of rGM-CSF (PeproTech) and 10 ng of rIL-4 (PeproTech) per ml (23). On day 4 of culture, immature DC were infected with rBCG at an indicated multiplicity of infection (MOI) and, on day 6 of culture, DC were used for further analyses of surface Ag and for mixed lymphocyte assays. The rMMP-II protein and BCG-derived cytosolic protein (BCC) were produced, as described previously (6, 24).

Vector construction and preparation of rBCG

For the preparation of rBCG that secretes HSP70-MMP-II fusion protein, a plasmid pMV-70M was constructed having a hygromycin resistance gene and origins of replication for *Escherichia coli* and mycobacteria. Briefly, the genomic DNA from BCG substrain Tokyo or *M. leprae* strain Thai-53 was purified by proteinase K digestion and phenol-chloroform extraction. The oligonucleotide primers for the amplication of the *hsp70* gene were FMb70Bal (5′-aaaTGGCCAtggctcgtgcggtcggg-3′; capital letters indicate a *BalI* site) and RMb70Eco (5′-aaaGAATTCcttggcctcccggccg-3′; capital letters indicate an *EcoRI* site). The primers for the Ag85B signal sequence of BCG were FMbAg85Bal (5′-tttTGGCCAtgacagacgtgagccgaaa-3′; capital letters indicate a *BalI* site) and RMbAg85 Eco120 (5′-aaaGAATTC cgcgcccgcggttgcc-3′; capital letters indicate an *EcoRI* site). The MMP-II sequence from *M. leprae* genomic DNA was amplified with FMMPEco4 (5′-aaaGAATTCcaaggtgatccggatgt-3′; capital letters indicate an *EcoRI* site) and RMMP Sal (5′-tgaGTCGACttaactcggcggccggga-3′; capital letters indicate a *SalI* site). The amplified products were digested with appropriate restriction enzymes and cloned into a *BalI-SalI*-digested parental pMV261 plasmid. For replacing the kanamycin resistance gene with a hygromycin resistance cassette, the *XbaI-NheI* fragment from pYUB854 (25) was cloned into *SpeI-NheI*-digested plasmids.

BCG substrain Tokyo was cultured in vitro using Middlebrook 7H9 broth (BD Biosciences) supplemented with 0.05% Tween 80 and 10% albumin-dextrose-catalase (BD Biosciences) or Sauton medium containing 0.05% Tween 80. Expression vectors were introduced into BCG by electroporation (26). Transformants were selected on Middlebrook 7H10 agar (BD Biosciences) plates. The BCG containing pMV-HSP70-MMP-II as an extrachromosomal plasmid is referred to as BCG-70M, and that containing pMV-261 is referred to as BCG-261H (BCG vector control). rBCGs were grown to a log phase, and stored at 10^8 CFU/ml at −80°C. Before the infection of DC, BCGs were counted by the colony assay method. There was no significant difference in growth in vitro between BCG-261H and BCG-70M.

Expression of the fusion protein HSP70-MMP-II

To verify the secretion of MMP-II and HSP70 from BCG-70M, the culture supernatant of BCG-70M, cultured for 20 days in Sauton medium, was collected, and concentrated using the Labscale TFF system (Millipore), after the supernatant was depleted of the cells by centrifugation. rMMP-II protein was used as a control for Western blotting. SDS-PAGE and electroblotting were conducted using standard methods (27). Western blotting was performed, as follows: a membrane having the transferred protein was blocked in 5% skim milk and then incubated with anti-MMP-II mAb 202-3 (IgG2a) or anti-mycobacterial HSP70 mAb (HyTest), which is not cross-reactive to mammalian HSP70 homologues. An alkaline-phosphatase-conjugated anti-mouse IgG Ab (BioSource International) was used as the secondary Ab. Color development was performed using NBT/5-bromo-4-chloro-3-indolyl phosphate detection reagent (Calbiochem).

Analysis of cell surface Ag

The expression of cell surface Ag on DC was analyzed using FACS Calibur. Dead cells were eliminated from the analysis based on staining with propidium iodide (Sigma-Aldrich), and 1×10^4 live cells were analyzed. For the analysis of the cell surface Ag, the following mAbs were used: a FITC-conjugated mAb against HLA-ABC (G46-2.6; BD Pharmingen), HLA-DR (L243; BD Biosciences), CD86 (FUN-1; BD Biosciences), CD83 (HB15a; Immunotech), and CD62L (Dreg 56; BD Biosciences), and a PE-conjugated mAb to CD8 (RPA-T8; BD Biosciences).

The expression of MMP-II on rBCG-infected DC was determined using a mAb (M270-13, IgM, κ) against MMP-II, which probably detects MMP-II in a complex with MHC molecules on the surface of DC (7), followed by a FITC-conjugated anti-mouse Igs Ab (Tago-immunologicals). For the inhibition of the intracellular processing of phagocytosed bacteria, DC were treated with 50 μM chloroquine (Sigma-Aldrich) for 2 h, washed, subsequently infected with BCG, and subjected to analyses of MMP-II surface expression. The intracellular production of perforin was assessed, as follows: unseparated naive T cells were stimulated with rBCG-infected DC for 5 days, and $CD8^+$ T cells were surface stained with a PE-labeled mAb to CD8, and fixed in 2% formaldehyde. Subsequently, the cells were permeabilized using permeabilizing solution (BD Biosciences), and stained with a FITC-conjugated mAb to perforin (δG9; BD Biosciences).

APC functions of DC

The ability of BCG-infected DC to stimulate T cells was assessed using an autologous DC-T cell coculture, as described previously (5, 23). Purification of $CD4^+$ and $CD8^+$ T cells was conducted by using negative isolation kits (Dynabeads 450; Dynal Biotech) (23). The purity of the $CD4^+$ and $CD8^+$ T cells was more than 95% when assessed using FACSCalibur. Naive $CD4^+$ and $CD8^+$ T cells were produced by further treatment of these T cells with a mAb to CD45RO, followed by beads coated with a mAb to goat anti-mouse IgGs (Dynal Biotech). The purity of both subsets of naive T cells was more than 97%. More than 98% of $CD45RA^+$ T cells expressed CCR7 molecule. Memory-type T cells were similarly produced by the treatment of cells with a mAb to CD45RA Ag. The purified responder cells (1×10^5 per well) were plated in 96-well round-bottom tissue culture plates, and DC were added to give the indicated DC:T cell ratio. Supernatants of DC-T cell cocultures were collected on day 4, and the cytokine levels were determined. In some cases, rBCG-infected DC were treated with a mAb to HLA-ABC (W6/32, mouse IgG2a, κ), HLA-DR (L243, mouse IgG2a, κ), CD86 (IT2.2, mouse IgG2b, κ; BD Biosciences), or MMP-II (M270-13), or with normal mouse IgG or IgM. The optimal concentration was determined in advance. Also, in some cases, immature DC

were treated with the indicated dose of chloroquine, brefeldin A (Sigma-Aldrich), or lactacystin (Sigma-Aldrich), and subsequently infected with BCG-70M. The optimal dose of these reagents was determined in advance.

Measurement of cytokine production

Levels of the following cytokines were measured: IFN-γ produced by $CD4^+$ and $CD8^+$ T cells, and IL-12p70, TNF-α, and IL-1β produced by DC stimulated for 24 or 48 h with rBCGs. The concentrations of these cytokines were quantified using the enzyme assay kits, Opt EIA Human ELISA Set (BD Biosciences). The murine mAb against TLR2 (clone 2392; IgG1) with antagonistic activity was obtained from Genentech. The optimal concentration of these mAbs was determined in advance.

Animal experiments

For the inoculation of mice, rBCG was cultured in Middlebrook 7H9 medium to a log phase of growth and stored at 10^8 CFU/ml at −80°C. Before the aliquots were used for inoculation, the concentration of viable bacilli was determined by plating on a Middlebrook 7H10 agar plate. Three 5-wk-old C57BL/6J mice (Japan CLEA) per group were inoculated s.c. with 0.1 ml of PBS or PBS containing 1×10^2 or 1×10^3 rBCGs. The animals were kept in specific pathogen-free conditions and supplied with sterilized food and water. Four weeks after the inoculation, the spleens were removed and the splenocytes were suspended at a concentration of 2×10^6 cells/ml in culture medium. The splenocytes were stimulated with an indicated concentration of rMMP-II, rHSP70 (HyTest), or BCC in triplicate in 96-well round-bottom microplates (14, 28). The individual culture supernatants were collected 3–4 days after the stimulation, and IFN-γ was measured using Opt EIA Mouse ELISA Set (BD Biosciences). The splenocytes obtained from C57BL/6 mice infected with rBCG were also subjected to the identification of T cell subsets responsible for IFN-γ production. The intracellular production of IFN-γ by $CD4^+$ T cells and $CD8^+$ T cells that were restimulated for 3 days in vitro with rMMP-II protein was assessed, as follows: cells were treated with Golgi Stop, and Golgi transport was inhibited for 4 h. Then the cells were surface stained with an allophycocyanin-labeled mAb to CD4 (RM4-5; BD Biosciences) and a PE-labeled mAb to CD8 (H35.17-2; BD Biosciences) in the presence of 7-aminoactinomycin D, after which the cells were washed with PBS containing 1% FCS and fixed in 1.6% formaldehyde. Subsequently, they were permeabilized using 0.1% saponin, and stained with a FITC-conjugated mAb to IFN-γ (XMG1.2; BD Biosciences) or isotype control IgG. Eight C57BL/6 mice per group were vaccinated with the indicated dose of BCG-261H or BCG-70M for 4 wk, and were challenged with 5×10^3/mouse *M. leprae* in footpad. Thirty-two weeks later, footpad was removed. The number of *M. leprae* grown in footpad was enumerated by Shepard method (29). Animal studies were reviewed and approved by the Animal Research Committee of Experimental Animals of the National Institute of Infectious Diseases, and were conducted according to their guidelines.

Statistical analysis

Student's *t* test was applied to determine statistical differences.

Results

Secretion of HSP70-MMP-II fusion protein from the rBCG (BCG-70M)

To verify the secretion of MMP-II protein from BCG-70M, culture filtrates of BCG transformants including BCG-261H (vector control) and BCG-70M were concentrated and examined by Western blotting analysis using mAbs to MMP-II and HSP70 (Fig. 1*A*). When probed by the MMP-II mAb, BCG-70M showed distinct band at 90-kDa equivalent to the molecular mass of the fusion protein comprising HSP70 and MMP-II, and control rMMP-II showed a 22-kDa band. Because BCG-Tokyo, a parental strain of BCG-70M and BCG-261H, has the gene encoding BCG-derived MMP-II, a faint 22-kDa band was observed in the culture filtrate of BCG-261H. In addition, when the culture filtrates were examined using the mAb to HSP70, the BCG-70M-derived filtrates expressed the 90-kDa protein, whereas the filtrates obtained from BCG-261H and rMMP-II protein did not express any obvious band. These results indicate that BCG-70M efficiently secreted the fusion protein comprising HSP70 and MMP-II. Furthermore, the HSP70-MMP-II fusion protein stimulated DC and induced a significant level of IL-12p70 production (Fig. 1*B*). To address the

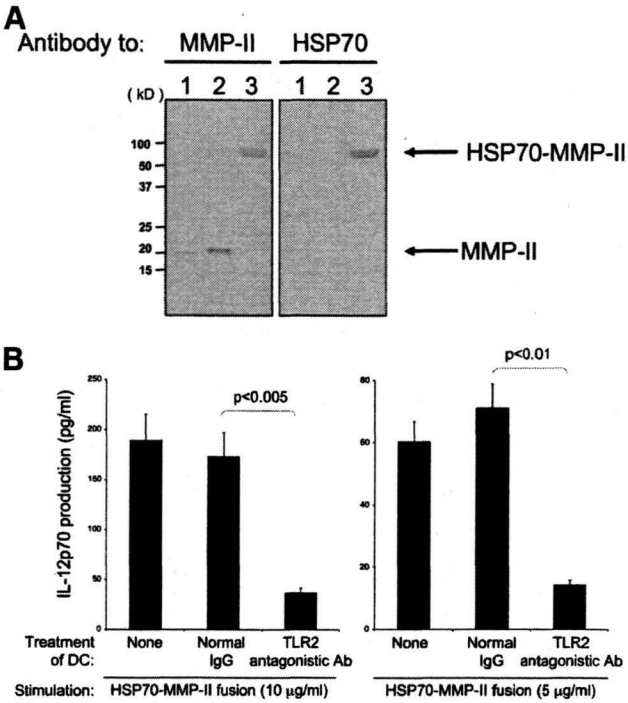

FIGURE 1. *A*, Western blotting analysis of protein secreted from BCG-70M. A mAb to either MMP-II or HSP70 was used to detect HSP70-MMP-II fusion protein. *Lane 1*, Culture filtrates of BCG-261H. *Lane 2*, rMMP-II protein. *Lane 3*, Culture filtrates of BCG-70M. *B*, Contribution of TLR2 to IL-12p70 production by DC by stimulation with HSP70-MMP-II fusion protein. PBMCs were obtained from one donor. Monocyte-derived DC were pretreated with either normal murine IgG or TLR2 antagonistic Ab (10 μg/ml) and subsequently stimulated with BCG-70M-derived HSP70-MMP-II fusion protein (10 or 5 μg/ml) for 24 h. The concentration of IL-12p70 was determined by the ELISA method. A representative of three separate experiments is shown. Assays were performed in triplicate, and the results are expressed as the mean ± SD. Titers were statistically compared using Student's *t* test.

contribution of TLR2 expressed on DC to the IL-12p70 production, DC were pretreated with an antagonistic Ab to TLR2 and subsequently stimulated with the fusion protein. More than 80% of IL-12p70 production was inhibited by the anti-TLR2 antagonistic Ab, whereas pretreatment of DC with normal murine IgG did not affect the level of production. Although BCG-261H induced IL-12p70 production from DC, production was only partially inhibited by the antagonistic Ab to TLR2 (data not shown).

Characteristics of BCG-70M

To define infectivity and survival in APCs, we examined the recovery rate of BCG-261H and BCG-70M. There was no significant difference between the two strains, and similar amounts of BCG were recovered as that of infected number (data not shown). Both HSP70 and MMP-II are known to be immunostimulators (6, 30). To see the effect of the secretion of HSP70-MMP-II fusion protein from BCG on the activation of DC, we analyzed the expression of surface Ags of BCG-infected DC (Fig. 2*A*). Both BCG-261H and BCG-70M enhanced the expression of HLA-ABC, HLA-DR, CD86, and CD83 Ags, but BCG-70M was significantly more efficient in up-regulating the expression of these molecules than BCG-261H. Furthermore, when various MOIs of BCG were used, a similar difference between BCG-261H and BCG-70M was observed (data not shown). Thus, BCG-70M phenotypically activated DC. Furthermroe, BCG-70M-infected DC significantly,

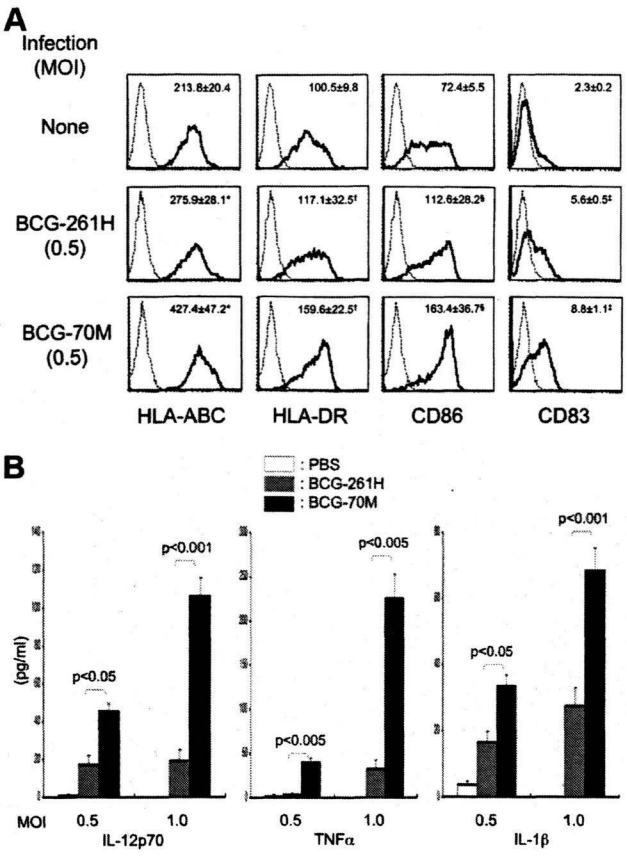

FIGURE 2. *A*, Up-regulated expression of APC-associated molecules on DC by infection with BCG-70M. PBMCs were obtained from one donor. Monocyte-derived immature DC were infected with either BCG-261H or BCG-70M at a MOI of 0.5 and cultured for another 2 days in the presence of rGM-CSF and rIL-4. The DC from day 5 were gated and analyzed. Dotted lines, isotype-matched control IgG; solid lines, the indicated test mAb. Representative results of three separate experiments are shown. The number in the *top right-hand corner* of each panel represents the mean ± SD for three independent experiments of the difference in mean fluorescence intensity between the control IgG and the test mAb. Titers were statistically compared using Student's *t* test. *, $p < 0.01$; †, $p < 0.05$; §, $p < 0.01$; ‡, $p < 0.05$. *B*, Cytokine production from DC stimulated with BCG. PBMCs were obtained from one donor. Monocyte-derived DC from 4 days of culture in the presence of rGM-CSF and rIL-4 were stimulated with the indicated dose of either BCG-261H or BCG-70M for 24 h. The concentration of the indicated cytokine was determined by the ELISA method. A representative of three separate experiments is shown. Assays were performed in triplicate, and the results are expressed as the mean ± SD. Titers were statistically compared using Student's *t* test.

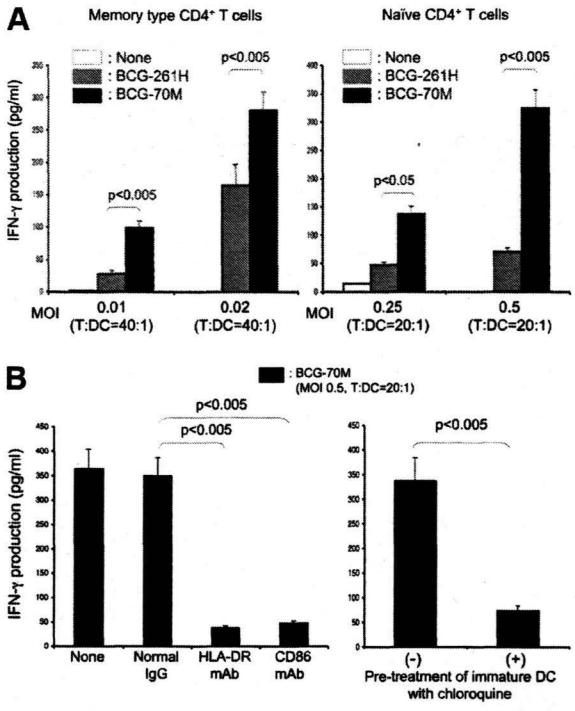

FIGURE 3. *A*, IFN-γ production from CD4+ T cells by stimulation with BCG. PBMCs were obtained from one donor. Monocyte-derived DC were infected with either BCG-261H or BCG-70M at the indicated MOI, and used as a stimulator of memory-type or naive CD4+ T cells in a 4-day culture. Responder CD4+ T cells (1×10^5) were stimulated with the indicated dose of BCG-infected DC. A representative of three separate experiments is shown. Assays were performed in triplicate, and the results are expressed as the mean ± SD. Titers were statistically compared using Student's *t* test. *B*, Inhibition of naive CD4+ T cell activation by the treatment of BCG-70M-infected DC with mAb or the treatment of immature DC with chloroquine. PBMCs were obtained from one donor. Monocyte-derived DC were infected with BCG-70M at a MOI of 0.5, and subsequently treated with 10 μg/ml mAb to HLA-DR, CD86 Ags, or normal murine IgG. Immature DC were treated with 50 μM chloroquine for 2 h and subsequently infected with BCG-70M at a MOI of 0.5. These DC were used as the stimulator of naive CD4+ T cells (1×10^5/well) at T:DC = 20:1. IFN-γ produced from T cells was measured. A representative of three separate experiments is shrown. Assays were performed in triplicate, and the results are expressed as the mean ± SD. Titers were statistically compared using Student's *t* test.

though faintly, expressed MMP-II on their surface, and the MMP-II expression was inhibited by the pretreatment of DC with chloroquine, an inhibitor of phagosomal acidification, before BCG-70M infection (data not shown). Moreover, when we examined the influence of BCG-70M infection in DC in terms of the production of proinflammatory cytokines, BCG-70M was superior to BCG-261H in the production of IL-12p70, TNF-α, and IL-1β (Fig. 2*B*). These results indicate again that BCG-70M more efficiently activated DC than did the parental BCG.

T cell activation by BCG-70M

Enhanced activation of DC may be closely associated with the efficient activation of both CD4+ and CD8+ T cell subsets. Because BCG-infected mitomycin C-treated DC were confirmed not to produce IFN-γ (data not shown), the T cell-activating ability of BCG-70M was assessed by using DC as APCs. Memory-type and naive CD4+ T cells were purified from healthy BCG-vaccinated individuals, and were stimulated with DC infected with rBCG (Fig. 3*A*). As expected, memory T cells responded more vigorously to DC infected with smaller dose of BCG than naive CD4+ T cells. Although both BCG-261H and BCG-70M stimulated memory and naive CD4+ T cells, BCG-70M induced a significantly higher level of IFN-γ production in both types of CD4+ T cells than BCG-261H. Note that high levels of IFN-γ could be produced from naive CD4+ T cells by BCG-70M. In addition, various MOIs and T:DC ratios were assessed, and a similar difference between BCG-261H and BCG-70M was observed (data not shown). To address the mechanism leading to the activation of naive CD4+ T cells, BCG-70M-infected DC were treated with mAbs to HLA-DR and CD86 molecules and subsequently used as a stimulator of the T cells. The IFN-γ production from naive CD4+ T cells was significantly inhibited by the surface treatment of BCG-70M-infected DC with the mAb to HLA-DR or CD86 (Fig. 3*B*), and similarly, IL-2 production from naive CD4+ T cells

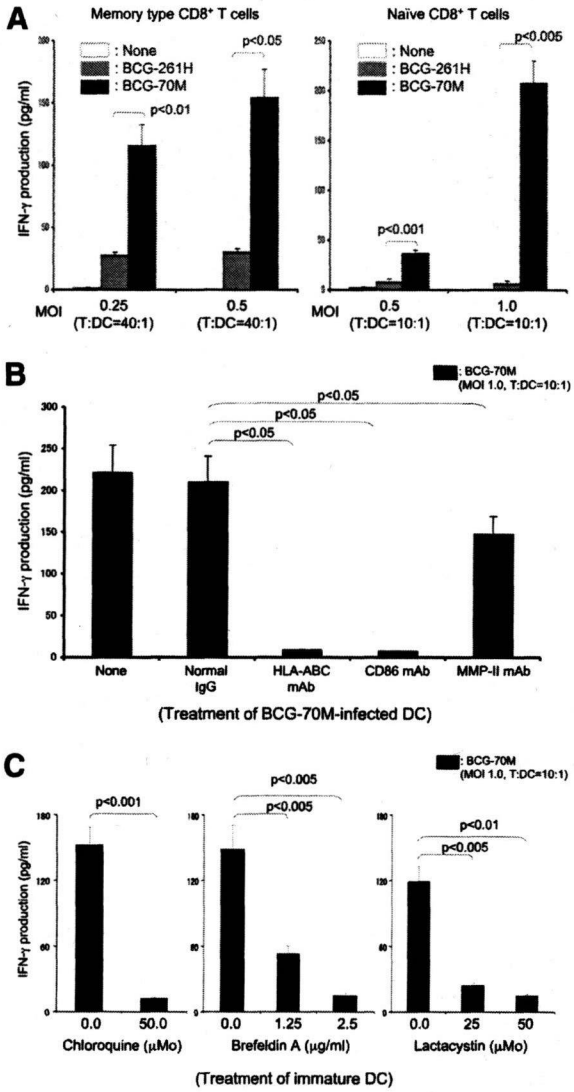

FIGURE 4. *A*, IFN-γ production from $CD8^+$ T cells by stimulation with BCG. PBMCs were obtained from one donor. Monocyte-derived DC were infected with either BCG-261H or BCG-70M at the indicated MOI, and used as a stimulator of memory-type or naive $CD8^+$ T cells in a 4-day culture. Responder $CD8^+$ T cells (1×10^5) were stimulated with the indicated dose of BCG-infected DC. A representative of three separate experiments is shown. Assays were performed in triplicate, and the results are expressed as the mean ± SD. Titers were statistically compared using Student's *t* test. *B*, Inhibition of naive $CD8^+$ T cell activation by the treatment of BCG-70M-infected DC with mAb. PBMCs were obtained from one donor. Monocyte-derived DC were infected with BCG-70M at a MOI of 1.0, and subsequently treated with 10 μg/ml mAb to HLA-ABC, CD86, or MMP-II (M270-13). The DC were used as the stimulator of naive $CD8^+$ T cells (1×10^5/well) at T:DC = 10:1. IFN-γ produced from the T cells was measured by the ELISA method. A representative of three separate experiments is shown. Assays were performed in triplicate, and the results are expressed as the mean ± SD. Titers were statistically compared using Student's *t* test. *C*, Effect of treatment of immature DC with reagents on the activation of naive $CD8^+$ T cells. PBMCs were obtained from one donor. Monocyte-derived immature DC were treated with the indicated dose of either chloroquine, brefeldin A, or lactacystin, and subsequently infected with BCG-70M at a MOI of 1.0. These DC were used as the stimulator of naive $CD8^+$ T cells (1×10^5/well) at T:DC = 10:1. IFN-γ produced from the T cells was measured. A representative of three separate experiments is shown. Assays were performed in triplicate, and the results are expressed as the mean ± SD. Titers were statistically compared using Student's *t* test.

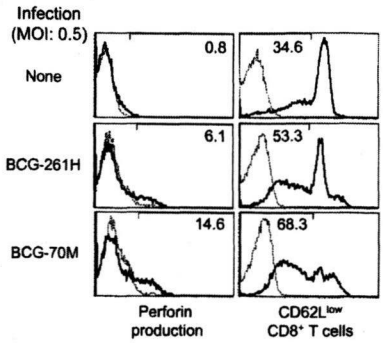

FIGURE 5. Influence of naive $CD4^+$ T cells on the activation of naive $CD8^+$ T cells. PBMCs were obtained from one donor. Monocyte-derived DC were infected with BCG (MOI 0.5) and cocultured with unseparated naive T cells (T:DC = 10:1) for 7 days. The stimulated $CD8^+$ T cells were gated and analyzed for perforin production and for expression of CD62L Ag. Numbers indicate either percentage of perforin-positive $CD8^+$ T cells or $CD62L^{low}$ $CD8^+$ T cells among $CD8^+$ T cell population. A representative of three separate experiments is shown.

was inhibited (data not shown). Furthermore, pretreatment of immature DC with chloroquine before infection with BCG-70M significantly inhibited the IFN-γ production from naive $CD4^+$ T cells (Fig. 3*B*). These results indicated that the secreted HSP70-MMP-II protein or BCG-70M itself may be processed in the DC, and some of the antigenic peptides were used for the stimulation of autologous Ag-specific naive $CD4^+$ T cells. Similarly, BCG-70M-infected DC stimulated memory $CD8^+$ T cells more efficiently than BCG-261H-infected DC, although a higher dose of BCG-70M was necessary to induce a similar level of IFN-γ production from $CD8^+$ T cells than the dose of BCG-70M required to produce the cytokine from memory $CD4^+$ T cells. As reported, BCG-261H did not activate naive $CD8^+$ T cells efficiently (15); however, BCG-70M-infected DC induced a significant level of IFN-γ production from naive $CD8^+$ T cells (Fig. 4*A*). Using a higher dose of BCG-70M (MOI 1.0) and a larger number of BCG-70M-infected DC (T:DC = 10:1), a high concentration (~200 pg/ml) of IFN-γ could be produced from naive $CD8^+$ T cells. In addition, various MOIs and T:DC ratios were assessed, and a similar difference between BCG-261H and BCG-70M was observed (data not shown). To clarify the mechanism leading to the activation of naive $CD8^+$ T cells by BCG-70M, BCG-70M-infected DC were treated with mAbs. Again, the activation of naive $CD8^+$ T cells by BCG-70M-infected DC was significantly inhibited by the treatment of the DC with the mAb to HLA-ABC or CD86. However, surface treatment of the DC with the mAb to MMP-II significantly, but only partially, inhibited the T cell activation (Fig. 4*B*). These results may indicate that BCG-70M-infected DC cross-primed naive $CD8^+$ T cells in an Ag-specific manner. To elucidate the mechanisms leading to the cross-presentation by BCG-70M-infected DC, we treated immature DC with various reagents in advance of the BCG-70M infection (Fig. 4*C*). On the pretreatment of DC with chloroquine, IFN-γ production from naive $CD8^+$ T cells was significantly inhibited, indicating that protein derived from BCG-70M was degraded in presumably the phagolysosome. Furthermore, on the pretreatment of DC with brefeldin A, an inhibitor of antegrade Golgi transportation, and lactacystin, an inhibitor of proteosomal protein degradation, IFN-γ production from naive $CD8^+$ T cells was inhibited significantly in a manner dependent on the concentration of the reagents. Because BCG-70M activated both naive $CD4^+$ T cells and naive $CD8^+$ T cells, we stimulated naive $CD8^+$ T cells with BCG-70M in the presence of the $CD4^+$ T cells (Fig. 5). The expression level of CD62L on some $CD8^+$ T cells was

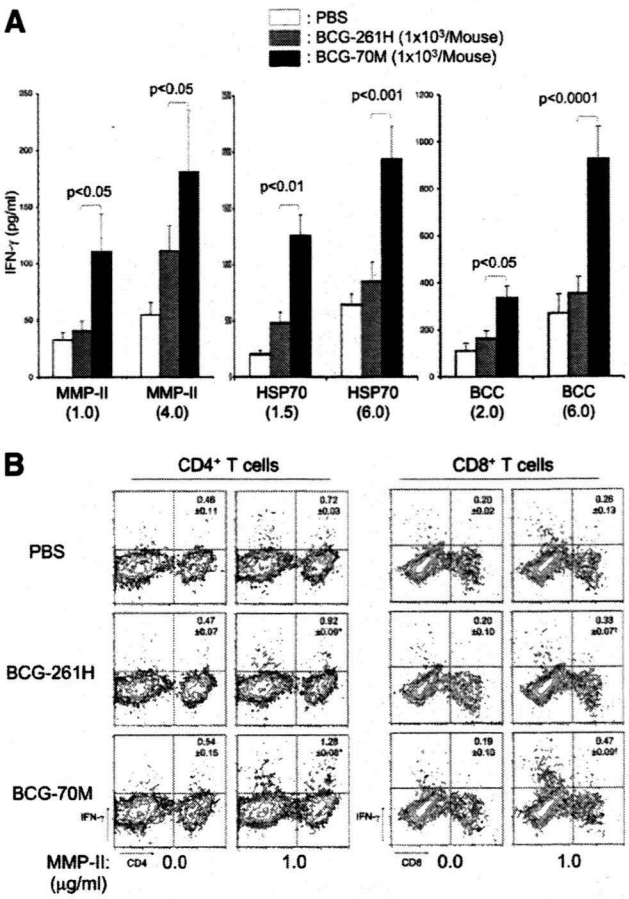

FIGURE 6. *A*, Production of memory-type T cells in C57BL/6 mice by infection with BCG. Five-week-old C57BL/6 mice were infected with 1×10^3 CFU/mouse of either BCG-261H or BCG-70M s.c. Four weeks after the inoculation, splenocytes (2×10^5 cells/well) were stimulated with the indicated dose of either MMP-II-, HSP70-, or BCG-derived cytosolic protein for 4 days, and IFN-γ produced in the cell supernatant was measured. Assays were performed in triplicate for each mouse, and the results of three mice per group are shown as the mean ± SD. Representative results of four separate experiments are shown. Titers were statistically compared using Student's *t* test. *B*, Intracellular IFN-γ production from $CD4^+$ T cells and $CD8^+$ T cells in C57BL/6 mice s.c. inoculated with BCG by secondary stimulation. Groups of 5-wk-old C57BL/6 mice were infected with 1×10^3/mouse BCG-261H or BCG-70M intradermally. Four weeks after the inoculation, splenocytes (2×10^5 cells/well) were stimulated with 1.0 μg/ml rMMP-II for 3 days. The $CD4^+$ T cells and $CD8^+$ T cells were gated separately and analyzed for intracellular production of IFN-γ. The number in the *top right-hand corner* of each panel represents the mean ± SD for three mice in the percentage of IFN-γ-producing cells among the gated T cell population. Representative results of four separate experiments are shown. Titers were statistically compared using Student's *t* test. *, $p < 0.05$; †, $p < 0.01$.

significantly reduced by stimulation with BCG-70M-infected DC, and a significant amount of intracellular perforin was produced in naive $CD8^+$ T cells by the stimulation. These changes were more efficiently induced by BCG-70M-infected DC than by BCG-261H-infected DC (Fig. 5). The $CD62L^{low}CD8^+$ T cells and perforin-producing $CD8^+$ T cells were not produced when naive $CD8^+$ T cells were stimulated in the absence of naive $CD4^+$ T cells (data not shown).

Memory T cell production by BCG-70M in vivo

Another important aspect to be studied is the production of Ag-specific memory T cells in vivo. C57BL/6 mice were infected with

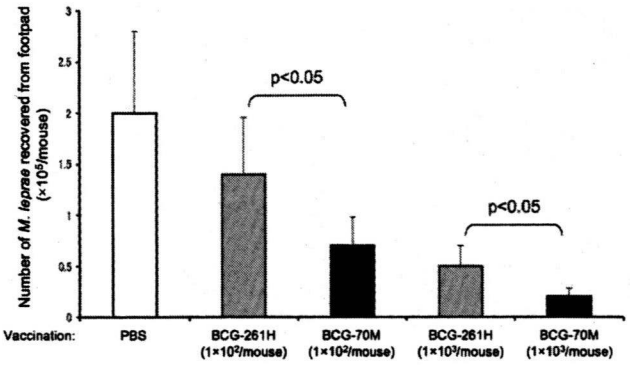

FIGURE 7. Inhibition of *M. leprae* multiplication by s.c. vaccination with BCG-70M. Five-week-old C57BL/6 mice (8 mice per group) were vaccinated with 1×10^2 or 1×10^3 CFU/mouse either BCG-261H or BCG-70M s.c., and were challenged with 5×10^3 bacilli/mouse *M. leprae* in footpad 4 wk after the vaccination. The number of *M. leprae* recovered from the footpad at 32 wk after the challenge was enumerated by Shepard's methods (29). Representative results of two separate experiments are shown. Titers were statistically compared using Student's *t* test.

1000 CFU/mouse rBCG for 4 wk, and their splenocytes were secondarily stimulated in vitro with rMMP-II protein, or recall Ags, like BCC (Fig. 6*A*). When a lower dose of MMP-II was used as a stimulator, only T cells obtained from BCG-70M-infected mice responded to the stimulator. Because BCG-Tokyo, the parental strain of the rBCGs, has the gene encoding MMP-II, a higher dose of *M. leprae*-derived MMP-II induced IFN-γ production from both T cells obtained from BCG-261H- and BCG-70M-inoculated mice; however, T cells from BCG-70M-infected mice more efficiently produced the cytokine than those from BCG-261H-infected mice. Also, T cells from BCG-70M-inoculated mice produced significantly higher level of IFN-γ than T cells from mice inoculated with BCG-261H on stimulation with HSP70 in vitro. The efficient generation of memory T cells responding to mycobacteria-derived Ags in mice infected with BCG-70M was confirmed, because only T cells from mice infected with BCG-70M significantly responded to BCC (Fig. 6*A*). To clarify the T cell subsets responsible for the IFN-γ production on secondary MMP-II stimulation, T cells producing the cytokine intracellulary were analyzed (Fig. 6*B*). Both $CD4^+$ T cells and $CD8^+$ T cells derived from not only non-BCG-inoculated mice, but also BCG-infected mice, produced intracellular IFN-γ by MMP-II stimulation. Both noninoculated and PBS-inoculated mice showed the similar responses (data not shown). However, significantly larger populations of both $CD4^+$ T cells (~1.3%) and $CD8^+$ T cells (~0.5%) obtained from BCG-70M-infected mice produced the cytokine. There were no $CD4^+$ T cells or $CD8^+$ T cells that were positively stained with the isotype control IgG (data not shown).

Effect of BCG-70M vaccination on the multiplication of M. leprae *in vivo*

C57BL/6 mice vaccinated with either BCG-261H or BCG-70M (1×10^2 or 1×10^3 CFU/mouse) for 4 wk were challenged with 5×10^3 of *M. leprae* in footpad. Thirty-two weeks later, footpad was removed and *M. leprae* recovered from the footpad was enumerated (Fig. 7). A total of 2×10^5 *M. leprae* was recovered from mice inoculated with PBS and challenged with *M. leprae*. Both mice inoculated with BCG-261H or BCG-70M inhibited the multiplication of *M. leprae* in the manner dependent on the dose of rBCG vaccinated; however, BCG-70M vaccination was significantly more efficient than BCG-261H vaccination in inhibiting the

multiplication, and only 2×10^4 *M. leprae* was recovered from mice vaccinated with 1×10^3 CFU/mouse BCG-70M.

Discussion

M. leprae is a representative mycobacterium among slow-growing prokaryotes, which needs 12–14 days for one division and 10–70 years for the manifestation of the disease, depending on the dose of bacilli entering the hosts. Host defense against *M. leprae* is chiefly conducted by adaptive immunity involving both $CD4^+$ and $CD8^+$ T cell subsets (3–5). Although $CD4^+$ T cells usually act at the initial phase of infection, $CD8^+$ T cells inhibit the multiplication of *M. leprae* in the chronic phase or when it is reactivated from a dormant state (31). Therefore, the vaccine should have an ability to competently activate not only $CD4^+$ T cells, but also $CD8^+$ T cells to produce memory T cells. To date, BCG is used as sole, but safe, vaccine against leprosy; however, nowadays, its efficacy is considered not so convincing (13). We have made several attempts to improve the potency of BCG, especially its immunostimulatory activities. We chiefly focused on achieving the fusion of BCG-infected phagosomes with lysosomes, without which the full and polyclonal activation of Ag-specific T cells cannot be expected. One approach we tried was the production of an *ure C*-deficient rBCG that successfully produces acidic phagosomes and facilitates their fusion with lysosomes (15, 28, 32, 33). Actually, the rBCG efficiently colocalized with lysosomes and effectively stimulated $CD4^+$ T cells when DC were targeted (28). However, it did not activate naive $CD8^+$ T cells. Then, we produced a second rBCG that secretes MMP-II (BCG-SM) in the phagosome (14). BCG-SM was useful in the activation of not only naive $CD4^+$ T cells, but also naive $CD8^+$ T cells to some extent (14). The T cell activation presumably occurs as a consequence of the translocation of the antigenic determinants of the secreted MMP-II to the cell surface, although the precise mechanism has not been clarified. Therefore, the intracellular secretion of immunodominant Ag by BCG is thought necessary to enhance the T cell-stimulating activity of BCG. However, BCG-SM vaccinations only partially inhibited the multiplication of *M. leprae* in the footpads of mice (our unpublished observation). These observations indicate the need for another rBCG capable of activating both naive $CD4^+$ and $CD8^+$ T cells more strongly.

Because the strong activation of naive $CD8^+$ T cells by mycobacteria required the cross-presentation of mycobacteria-derived Ags to $CD8^+$ T cells, in this study, we used BCG-derived HSP70 as a mediator facilitating the cross-presentation by DC, because HSPs of both mammalian host cells and bacterial origin are reported to have chaperone activity (34) and can effectively prime a cytolytic response (35). The usefulness of HSP65 as a convincing stimulator of $CD8^+$ T cells was revealed in animal studies to develop vaccine against *M. tuberculosis* (36). A DNA vaccine containing the *hsp65* gene activated naive $CD8^+$ T cells, and consequently inhibited the development of tuberculosis, although precisely how was not clarified. Our newly constructed rBCG (BCG-70M) secreted a fusion protein comprising HSP70 and MMP-II in vitro in the absence of any exogenous secretion signal. The secretion of HSP70-MMP-II fusion was confirmed by Western blotting analyses (Fig. 1*A*) and by the surface expression of MMP-II on DC (data not shown). The exact mechanism leading to the secretion of the fusion protein from BCG-70M is not known, but the secretion could be due to the inherent characteristics of HSP70 to be secreted (16, 37). Although we tried to enhance the secreting activity of BCG-70M by additionally inserting *M. tuberculosis*-derived secretion signal to BCG-70M, the secretion efficacy was rather inhibited and the construct stimulated naive T cells less efficiently than BCG-70M (data not shown).

BCG-70M secreted a 90-kDa fusion protein composed of HSP70 and MMP-II (14). The activation of naive $CD8^+$ T cells by BCG-70M was only partially inhibited by the treatment of DC with the mAb to MMP-II. Therefore, it can be speculated that BCG-70M activated $CD8^+$ T cells polyclonally by using various epitopes, originating from MMP-II, HSP70, or other Ags of BCG, because T cells from BCG-70M-infected mice vigorously responded to MMP-II, HSP70, and BCG-derived cytosolic protein (Fig. 6*A*). Therefore, HSP70 may alter the clonality of responding $CD8^+$ T cells, and the production of such polyclonal Ag-specific $CD8^+$ T cells might be beneficial for the broad coverage of a heterogenous MHC population.

BCG-70M induced higher level of cytokine production, including IL-12p70, TNF-α, and IL-1β, than the vector control BCG. The enhanced cytokine production by BCG-70M could be due to the intracellular secretion of HSP70 as a part of the fusion protein by the BCG. MMP-II can ligate TLR2 (6), but HSP70 is also known to bind TLRs (38); thus, the secreted HSP70-MMP-II protein seems to activate DC strongly. The contribution of TLR2 to cytokine production was confirmed by the inhibition of IL-12p70 production by antagonistic Ab to TLR2. The cytokines released from DC by BCG-70M stimulation could facilitate skewing of the direction of T cell activation to type 1 and induce the efficient and strong production of IFN-γ from naive $CD8^+$ T cells.

HSPs play a varied role in enhancing the ability of APCs to stimulate T cells (39). For the activation of Ag-specific $CD4^+$ and $CD8^+$ T cells, peptides should be loaded onto the corresponding MHC pathways. For the loading of BCG-derived Ags on these pathways, the proteins secreted from phagocytozed BCG should be transported to functional lysosomes. In the phagolysosome, some portions of HSP70-MMP-II fusion protein could be degraded, but the rest would be sequestrated into the cytosol, where they are degraded and used for cross-priming $CD8^+$ T cells. BCG-70M-infected DC expressed derivatives of MMP-II and the other proteins on their surface, and they activated both naive $CD4^+$ T cells and naive $CD8^+$ T cells. However, both MMP-II expression on DC and the activation of the T cells by DC were inhibited by the pretreatment of DC with chloroquine (24, 40). These results indicate that secreted HSP70-MMP-II fusion protein was efficiently processed in lysosomes and its derivatives are used for the activation of both subsets of naive T cells. When naive $CD8^+$ T cells were stimulated by BCG-70M in the presence of naive $CD4^+$ T cells, $CD62L^{low}CD8^+$ T cells and perforin-producing $CD8^+$ T cells were efficiently produced. The activation of naive T cells was confirmed by the production of memory-type T cells by BCG-70M infection to unprimed mice, because both $CD4^+$ and $CD8^+$ T cell subsets from BCG-70M-infected mice responded to the restimulation with MMP-II in vitro. Furthermore, BCG-70M significantly and more efficiently inhibited the multiplication of *M. leprae*, which were challenged in footpad of mice, than BCG-261H.

There are two pathways of cross-presentation, as follows: cytosolic (ER-Golgi-dependent) and vacuolar pathways (20). It is known that HSP can enhance both pathways (20). In the present study, IFN-γ production from naive $CD8^+$ T cells was largely blocked by the treatment of DC with brefeldin A, an inhibitior of antegrade Golgi transportation and of TAP-dependent transportation, and also with lactacystin, a proteosomal protein degradation blocker (20, 40). Therefore, it can be presumed that the fusion protein was sequestered into the cytosol from the lysosome, degraded in the proteosome, and used for loading on MHC class I molecules through the TAP-dependent pathway. Furthermore, it has been reported that proteins that are intracellularly secreted are usually processed by a cytosolic (ER-Golgi-dependent) pathway, and DC prefer this pathway for cross-priming $CD8^+$ T cells with

protein Ag (20). Our present observations seem to fit well with these previous findings. Therefore, we concluded that BCG-70M activates naive CD8$^+$ T cells through the ER-Golgi-dependent cytosolic cross-presentation pathway. However, *M. tuberculosis*-derived HSP70 activated T cells through a post-Golgi, proteosomal-independent mechanism, and both brefeldin A and lactacystin may inhibit vacuolar pathway in some cases (20). Also, the vacuolar pathway is used more frequently by macrophages (20). Therefore, the possibility that BCG-70M may also use the post-Golgi pathway in vivo cannot be ruled out.

Taken together, in this study, we constructed a rBCG that secretes HSP70-MMP-II fusion protein, which effectively activates not only DC, but also naive T cells. Therefore, the combination of HSP70 and MMP-II may be useful for stimulating both subsets of naive T cells.

Acknowledgments

We acknowledge the contribution of N. Makino in the preparation of the manuscript. We also thank Y. Harada for her technical support, and the Japanese Red Cross Society for kindly providing PBMCs from healthy donors.

Disclosures

The authors have no financial conflict of interest.

References

1. Hagge, D. A., N. A. Ray, J. L. Krahenbuhl, and L. B. Adams. 2004. An in vitro model for the lepromatous leprosy granuloma: fate of *Mycobacterium leprae* from target macrophages after interaction with normal and activated effector macrophages. *J. Immunol.* 172: 7771–7779.
2. Ridley, D. S., and W. H. Jopling. 1966. Classification of leprosy according to immunity: a five-group system. *Int. J. Lepr. Other Mycobact. Dis.* 34: 255–273.
3. Modlin, R. L., J. Melancon-Kaplan, S. M. M. Young, C. Piemez, H. Kino, J. Convit, T. H. Rea, and B. R. Bloom. 1988. Learning from lesions: patterns of tissue inflammations in leprosy. *Proc. Natl. Acad. Sci. USA* 85: 1213–1217.
4. Ramasesh, N., L. B. Adams, S. G. Franzblau, and J. L. Krahenbuhl. 1991. Effects of activated macrophages on *Mycobacterium leprae*. *Infect. Immun.* 59: 2864–2869.
5. Hashimoto, K., Y. Maeda, H. Kimura, K. Suzuki, A. Masuda, M. Matsuoka, and M. Makino. 2002. Infection of *M. leprae* to monocyte derived dendritic cells and its influence on antigen presenting function. *Infect. Immun.* 70: 5167–5176.
6. Maeda, Y., T. Mukai, J. Spencer, and M. Makino. 2005. Identification of immunomodulating agent from *Mycobacterium leprae*. *Infect. Immun.* 73: 2744–2750.
7. Makino, M., Y. Maeda, and N. Ishii. 2005. Immunostimulatory activity of major membrane protein-II from *Mycobacterium leprae*. *Cell. Immunol.* 233: 53–60.
8. Sieling, P. A., D. Jullien, M. Dahlem, T. F. Tedder, T. H. Rea, R. L. Modlin, and S. A. Porcelli. 1999. CD1 expression by dendritic cells in human leprosy lesions: correlation with effective host immunity. *J. Immunol.* 162: 1851–1858.
9. Seiling, P. A., M. T. Ochoa, D. Jullien, D. S. Leslie, S. Sabet, J. P. Rosat, A. E. Burdick, T. H. Rea, M. B. Brenner, S. A. Porcelli, and R. A. Modlin. 2000. Evidence for human CD4$^+$ T cells in the CD1-restricted repertoire: derivation of mycobacteria reactive T cells from leprosy lesions. *J. Immunol.* 164: 4790–4796.
10. Lombardi, C., E. S. Pedrazzani, J. C. Pedrazzani, P. F. Filho, and F. Zicker. 1996. Protective efficacy of BCG against leprosy in San Paulo. *Bull. Pan Am. Health Organ.* 30: 24–30.
11. Ponnighaus, J. M., P. E. Fine, J. A. Sterne, R. J. Wilson, E. Msosa, P. J. Gruer, P. A. Jenkins, S. B. Lucas, N. G. Liomba, and L. Bliss. 1992. Efficacy of BCG vaccine against leprosy and tuberculosis in northern Malawi. *Lancet* 14: 636–639.
12. Sharma, P., R. Mukherjee, G. P. Talwar, K. G. Sarathchandra, R. Walia, S. K. Parida, R. M. Pandey, R. Rani, H. Kar, A. Mukherjee, et al. 2005. Immunoprophylactic effects of the anti-leprosy *Mw* vaccine in household contacts of leprosy patients: clinical field trails with a follow up of 8–10 years. *Lepr. Rev.* 76: 127–143.
13. Setia, M. S., C. Steinmaus, C. H. Ho, and G. W. Rutherford. 2006. The role of BCG in prevention of leprosy: a meta-analysis. *Lancet Infect. Dis.* 6: 162–170.
14. Makino, M., Y. Maeda, and K. Inagaki. 2006. Immunostimulatory activity of recombinant *Mycobacterium bovis* BCG that secretes major membrane protein II of *Mycobacterium leprae*. *Infect. Immun.* 74: 6264–6271.
15. Grode, L., P. Seiler, S. Baumann, J. Hess, V. Brinkmann, A. N. Eddine, P. Mann, C. Goosmann, S. Bandermann, D. Smith, et al. 2005. Increased vaccine efficacy against tuberculosis of recombinant *Mycobacterium bovis* bacille Calmette-Guerin mutants that secrete listeriolysin. *J. Clin. Invest.* 115: 2472–2479.
16. Horwitz, M. A., B. W. Lee, B. J. Dillon, and G. Harth. 1995. Protective immunity against tuberculosis induced by vaccination with major extracellular proteins of *Mycobacterium tuberculosis*. *Proc. Natl. Acad. Sci. USA* 92: 1530–1534.
17. Binder, R. J., and P. K. Srivastava. 2005. Peptides chaperoned by heat-shock proteins are necessary and sufficient source of antigen in the cross-priming of CD8$^+$ T cells. *Nat. Immunol.* 6: 593–599.
18. Flechtner, J. B., K. P. Cohane, S. Mehta, P. Slusarewicz, A. K. Leonard, B. H. Barber, D. L. Levey, and S. Andjelic. 2006. High-affinity interactions between peptides and heat shock protein 70 augment CD8$^+$ T lymphocyte immune responses. *J. Immunol.* 177: 1017–1027.
19. Tobian, A. A. R., D. H. Canaday, W. H. Boom, and C. V. Harding. 2004. Bacterial heat shock proteins promote CD91-dependent class I MHC cross-presentation of chaperoned peptide to CD8$^+$ T cells by cytosolic mechanisms in dendritic cells versus vacuolar mechanisms in macrophages. *J. Immunol.* 172: 5277–5286.
20. Tobian, A. A. R., C. V. Harding, and D. H. Canaday. 2005. *Mycobacterium tuberculosis* heat shock fusion protein enhances class I MHC cross-processing and -presentation by B lymphocytes. *J. Immunol.* 174: 5209–5214.
21. Makino, M., and M. Baba. 1997. A cryopreservation method of human peripheral blood mononuclear cells for efficient production of dendritic cells. *Scand. J. Immunol.* 45: 618–622.
22. Wakamatsu, S., M. Makino, C. Tei, and M. Baba. 1999. Monocyte-driven activation-induced apoptotic cell death of human T-lymphotropic virus type I-infected T cells. *J. Immunol.* 163: 3914–3919.
23. Makino, M., S. Shimokubo, S. Wakamatsu, S. Izumo, and M. Baba. 1999. The role of human T-lymphotropic virus type 1 (HTLV-1)-infected dendritic cells in the development of HTLV-1-associated myelopathy/tropical spastic paraparesis. *J. Virol.* 73: 4575–4581.
24. Maeda, Y., M. Gidoh, N. Ishii, C. Mukai, and M. Makino. 2003. Assessment of cell mediated immunogenicity of *Mycobacterium leprae*-derived antigens. *Cell. Immunol.* 222: 69–77.
25. Bardarov, S., S. Bardarov, Jr., M. S. Pavelka, Jr., V. Sambandamurthy, M. Larsen, J. Tufariello, J. Chan, G. Hatfull, and W. R. Jacobs, Jr. 2002. Specialized transduction: an efficient method for generating marked and unmarked targeted gene disruptions in *Mycobacterium tuberculosis*, *M. bovis* BCG and *M. smegmatis*. *Microbiology* 148: 3007–3017.
26. Snapper, S. B., L. lugosi, A. Jekkel, R. E. Melton, T. Kieser, B. R. Bloom, and W. R. Jacobs, Jr. 1988. Lysogeny and transformation in mycobacteria: stable expression of foreign genes. *Proc. Natl. Acad. Sci. USA* 85: 6987–6991.
27. Sambrook, J., and D. W. Russell. 2001. *Molecular Cloning: A Laboratory Manual*, 3rd Ed. Cold Spring Harbor Laboratory Press, Cold Spring Harbor.
28. Mukai, T., Y. Maeda, T. Tamura, Y. Miyamoto, and M. Makino. 2008. CD4$^+$ T-cell activation by antigen-presenting cells infected with urease-deficient recombinant *Mycobacterium bovis* bacillus Calmette-Guérin. *FEMS Immunol. Med. Microbiol.* 53: 96–106.
29. Shepard, C. C., and D. H. McRae. 1968. A method for counting acid-fast bacteria. *Int. J. Lepr. Other Mycobact. Dis.* 36: 78–82.
30. Wang, Y., T. Whittall, E. McGowan, J. Younson, C. Kelly, L. A. Bergmeier, M. Singh, and T. Lehner. 2005. Identification of stimulating and inhibitory epitopes within the heat shock protein 70 molecule that modulate cytokine production and maturation of dendritic cells. *J. Immunol.* 174: 3306–3316.
31. Kaufmann, S. H. E., and A. J. McMichael. 2005. Annulling a dangerous liaison: vaccination strategies against AIDS and tuberculosis. *Nat. Med.* 11: S33–S44.
32. Clements, D. I., B. Y. Lee, and M. A. Horwitz. 1995. Purification, characterization, and genetic-analysis of *Mycobacterium tuberculosis* urease, a potentially critical determinant of host-pathogen interaction. *J. Bacteriol.* 177: 5644–5652.
33. Reyrat, J. M., F. X. Berthet, and B. Gicquel. 1995. The urease locus of *Mycobacterium tuberculosis* and its utilization for the demonstration of allelic exchange in *Mycobacterium bovis* bacillus Calmette-Guérin. *Proc. Natl. Acad. Sci. USA* 92: 8768–8772.
34. Flynn, G. C., T. G. Chappell, and J. E. Rothman. 1989. Peptide binding and release by proteins implicated as catalysts of protein assembly. *Science* 245: 385–390.
35. Moroi, Y., M. Mayhew, J. Trcka, M. H. Hoe, Y. Takechi, F. U. Hartl, J. E. Rothman, and A. N. Houghton. 2000. Induction of cellular immunity by immunization with novel hybrid peptides complexed to heat shock protein 70. *Proc. Natl. Acad. Sci. USA* 97: 3485–3490.
36. Yoshida, S., T. Tanaka, Y. Kita, S. Kuwayama, N. Kanamura, Y. Muraki, S. Hashimoto, Y. Inoue, M. Sakatani, B. Kobayashi, et al. 2006. DNA vaccine using hemagglutinating virus of Japan-liposome encapsulating combination encoding mycobacterial heat shock protein 65 and interleukin-12 confers protection against *Mycobacterium tuberculosis* by T cell activation. *Vaccine* 24: 1191–1204.
37. Belisle, J. T., V. D. Vissa, T. Sievert, K. Takayama, P. J. Brennan, and G. S. Besra. 1997. Role of the major antigen of *Mycobacterium tuberculosis* in cell wall biogenesis. *Science* 276: 1420–1422.
38. Asea, A., M. Rehli, E. Kabingu, J. A. Boch, O. Bare, P. E. Auron, M. A. Stevenson, and S. K. Calderwood. 2002. Novel signal transduction pathway utilized by extracellular HSP70: role of Toll-like receptor (TLR) 2 and TLR4. *J. Biol. Chem.* 277: 15028–15304.
39. Wang, Y., C. G. Kelly, M. Singh, E. G. McGowan, A. S. Carrara, L. A. Bergmeier, and T. Lehner. 2002. Stimulation of Th1-polarizing cytokines, C-C chemokines, maturation of dendritic cells, and adjuvant function by the peptide binding fragment of heat shock protein 70. *J. Immunol.* 169: 2422–2429.
40. Schiavo, R., D. Baatar, P. Olkhaund, F. E. Indig, N. Restifo, D. Taub, and A. Biragyn. 2006. Chemokine receptor targeting efficiently directs antigens to MHC class I pathways and elicits antigen-specific CD8$^+$ T-cell responses. *Blood* 107: 4597–4605.

Tohoku J. Exp. Med., 2009, **219**, 00-00

Establishment of A Guinea Pig Model of Latent Tuberculosis with GFP-introduced *Mycobacterium Tuberculosis*

Isamu Sugawara,[1] Tadashi Udagawa,[1] Toshiaki Aoki[1] and Satoru Mizuno[1]

[1]The Research Institute of Tuberculosis, Japan Anti-Tuberculosis Association, Kiyose, Tokyo, Japan

There exists latent tuberculosis, in which small numbers of tubercle bacilli remain viable in the host without visible granulomatous lesions. As few data exist on the mechanisms of latent tuberculosis, it is important to examine latent tuberculosis in terms of pathogenesis and efficacy of chemotherapy. As a first step, we used green fluorescent protein (GFP)-introduced H37Rv *Mycobacterium tuberculosis* to establish latent tuberculosis in the guinea pig that provides one of the best animal models of tuberculosis. We inoculated the guinea pigs subcutaneously with 100 or 1,000 colony-forming unit (CFU) of tubercle bacilli. During the 300-day follow-up period after infection, there were no clinical signs of disease, suggesting a lack of visible granulomatous lesions. In fact, upon necropsy, no macroscopic tuberculous lesions were recognized, but histopathological examination of the lung, spleen and liver revealed microgranulomas consisting of epithelioid macrophages and lymphocytes without central necrosis. Importantly, photon imaging visualized granulomatous lesions corresponding to these histologically apparent microgranulomas. Tuberculin skin testing of infected guinea pigs showed strong positivity (≥ 10 mm induration) until the end of the experiments. Real-time PCR analysis showed a significant increase in the expression levels of interferon-γ, tumor necrosis factor-α, interleukin-12, and inducible nitric oxide synthase mRNAs in infected lung tissues after 300 days ($P < 0.01$). As human samples are hardly available to study latent tuberculosis, our guinea pig model would be useful for examining the pathogenesis and molecular mechanisms of latent tuberculosis as well as for monitoring the results of chemotherapy with green fluorescence emission of tubercle bacilli.

——— GFP-H37Rv; latent infection; guinea pigs; *Mycobacterium tuberculosis*; photon imaging.

Tohoku J. Exp. Med., 2009, **219** (3), 000-000.

Most cases of adult tuberculosis occur in individuals who have been previously exposed to *Mycobacterium tuberculosis* and have developed a localized and self-healing inflammatory reaction. In most of the individuals the inflammatory reaction is spontaneously contained; often it calcifies and persists for the remainder of the person's life (Medlar 1950). Small numbers of tubercle bacilli are thought to remain viable for life in a condition known as latent or dormant tuberculosis (Lurie 1950). However, it is almost impossible to understand the mechanism and pathogenesis of human latent tuberculosis because of the difficulty in obtaining suitable samples.

To overcome this difficulty several mouse models of latent tuberculosis have been proposed (McCune et al. 1956; Orme 1987; Phyu et al. 1998). Whether or not these murine models truly represent latent human tuberculosis remains controversial, but two models have been proposed: a low-dose model and the Cornell model. The low-dose model has the marked advantage of mimicking natural latency in the sense that it relies solely on the host immune response for control of the infection, but it has the disadvantage of a high bacillary burden that is unlike that found in human latent *M. tuberculosis* infection (Orme 1987). The drug-induced Cornell model of latent tuberculosis has the advantage of achieving very low or undetectable numbers of bacilli and maintaining those low levels for many weeks in a pattern analogous to that in human latent infection, but it has the disadvantage of artificially inducing latency. Therefore, Cornell model variants have been proposed (Scanga et al. 1999).

The guinea pig provides one of the best animal models for tuberculosis. Recently, a guinea pig model of latent or dormant infection with *M. tuberculosis* was created using a streptomycin-auxotrophic mutant of *M. tuberculosis* and streptomycin (Kashino et al. 2008). Although this model is relatively reproducible, it is complicated in that it uses *M. tuberculosis* 18b (Hashimoto 1955; Shi et al. 2007), which only a limited number of laboratories possess. We previously reported the photon imaging of pulmonary granulomas induced by *Mycobacterium tuberculosis* H37Rv strain expressing green fluorescent protein (GFP) (Sugawara et al. 2006), showing that pulmonary granulomas more than 1 mm in diameter are localized clearly by the photon imager. We therefore considered it possible to detect latent granulo-

Received August 27, 2009; revision accepted for publication September 28, 2009. doi:10.1620/tjem.219.000

Correspondence: Isamu Sugawara, The Research Institute of Tuberculosis, Japan Anti-Tuberculosis Association, 3-1-24 Matsuyama, Kiyose, Tokyo 204-0022, Japan.

e-mail: sugawara@jata.or.jp

mas by photon imaging.

To expand the limited amounts of data currently available on the mechanisms of latent tuberculosis in guinea pigs, we used GFP-H37Rv to develop a low-dose model of guinea pig *M. tuberculosis* latent infection. Upon necropsy, no macroscopic tuberculous lesions were recognized, but histopathological examination of organs revealed microgranulomas consisting of epithelioid macrophages and lymphocytes without central necrosis. Interestingly, the photon imager visualized granulomatous lesions that corresponded to the histologically apparent granulomas. Our guinea pig model should be useful for examining the molecular mechanisms of latent tuberculosis and for monitoring chemotherapy of latent tuberculosis utilizing green fluorescence emission.

Materials and Methods

Bacterial strain and animal infection

Mycobacterium tuberculosis H37Rv strain (ATCC 25618) was transformed with the heat shock protein (HSP) 60 promoter-GFP mut 3.1 M to obtain a stable GFP-H37Rv mutant (Sugawara et al. 2006). This mutant remains stable for a year after subcutaneous administration to C57BL/6 mice, and there is no significant difference in growth rate or virulence between H37Rv and GFP-H37Rv (Sugawara et al. 2006).

Outbred female Hartley guinea pigs (average weight 250 g) purchased from SLC Co., Shizuoka, Japan, were infected subcutaneously with 100 or 1,000 CFU of GFP-H37Rv (ten in each group). Ten uninfected outbred female Hartley guinea pigs were also used. All experiments were conducted in compliance with the Guidelines for the Animal Care and Use Committee of The Research Institute of Tuberculosis.

Histopathology

For histopathological examination, the guinea pig's lungs, spleen, hilar lymph nodes, and liver were removed and embedded in paraffin. Sections 4 μm thick were cut, formaldehyde-fixed, and stained with hematoxylin and eosin or by the Ziehl-Neelsen method for acid-fast bacilli (AFB) (Sugawara et al. 2004).

Colony-forming unit (CFU)

At different time points after infection (6 months and 10 months), animals were euthanatized and their lungs and spleen removed. Organ homogenates were prepared in phosphate-buffered saline (PBS) and plated at 10-fold serial dilution on 1% Ogawa slant media. The plated agar was incubated at 37°C for 4 weeks and the CFU were counted 4 weeks later (Yamada et al. 2001; Sugawara et al. 2006).

Delayed type hypersensitivity reaction

Tuberculin skin tests were performed by intradermal injection of pure protein derivative (PPD) (50 μl/guinea pig, 50 μg/1 mL, Japan BCG Labs., Tokyo, Japan) into a small shaved area of the skin of the back. Twenty-four hours later transverse diameters of induration reaction were measured in millimeters (Sugawara et al. 2006).

Immunohistochemistry

Immunohistochemistry was performed with avidin-biotin-peroxidase complex (ABC), as described in detail previously (Hsu et al. 1981). Anti-BCG antibody (Dakopatts, Copenhagen, Denmark) was used at a final concentration of 10 μg/mL (Sugawara et al. 1998) to visualize BCG-related antigens. For negative-control slides, all these steps were repeated, but with non-immune serum substituted for the primary antibody.

Real-time PCR

The remaining portions of the right lower lobes of the lungs and of the spleen were used for reverse transcription (RT) polymerase chain reaction (PCR) analysis to examine the expression levels of several cytokine mRNAs during GFP-H37Rv infection. These samples were snap-frozen in liquid nitrogen and stored at –85°C until use. RNA extraction was performed as described previously (Yamada et al. 2005). Briefly, the frozen tissues were homogenized in a microcentrifuge tube with an autoclaved disposable 1,000-μL tip cooled down at 4°C by being dipped in liquid nitrogen. The homogenates were then treated with 1 mL of TRIzol reagent (Invitrogen Japan Co., Tokyo, Japan), as specified by the manufacturer. After RNA isolation, the total RNA concentration was measured with a spectrophotometer, and the agarose gel electrophoresis pattern of the total RNA was examined. The total RNAs were reverse-transcribed into cDNA with Moloney murine leukemia virus reverse transcriptase (Invitrogen). ABI TaqMan Gene Expression Assay was used for relative quantification of the expression of interferon (IFN)-γ, tumor necrosis factor (TNF)-α, interleukin (IL)-10, IL-12, and inducible nitric oxide synthase (iNOS) mRNAs. A TaqMan Rodent glyceraldehydes-3-phophate dehydrogenase (GAPDH) Control Reagents set was used for normalization for data analysis. Real-time RT-PCR was performed according to the instructions for the ABI PRISM 7900HT Sequence Detection System (Applied BioSystems Inc., California, USA). Data were analyzed by the $\Delta\Delta C_T$ method using the ABI PRISM Sequence Detection System software package (version 2.1; Applied BioSystems) on a Windows 2000 operating system. The results obtained from GFP-H37Rv-infected and control guinea pigs were expressed relative to those from uninfected guinea pigs, which were calibrated against the expression of an internal control gene (GAPDH) (Yamada et al. 2007).

Photon imaging

Guinea pigs infected with GFP-H37Rv were scanned for green fluorescence by using a Φ imager (photon imager, Biospace Mesures, Paris, France; or NightOwl LB 981 Molecular Light Imager, Berthold Technologies, Germany). This imager is based on a third-generation GaAs intensified charge-coupled device (ICCD) camera that allows real-time photon counting over a wide spectral range (wavelength 400 to 900 nm). The imager uses an ICCD chip to amplify every photon up to 10^6 light spots in a detector. The detection conditions of this imager were as follows: spatial resolution, equivalent to 1,080 × 1,440 pixels CCD; dynamics, 2,000 counts pixel^{-1} min^{-1}; excitation wavelength, 485 nm; emission wavelength, 535 nm (Sugawara et al. 2006; Hyoudou et al. 2007).

Statistical analysis

All values were expressed as means ± S.D. and compared by using Student's *t*-test. For all statistical analyses, the level of statistical significance was set at $P < 0.01$.

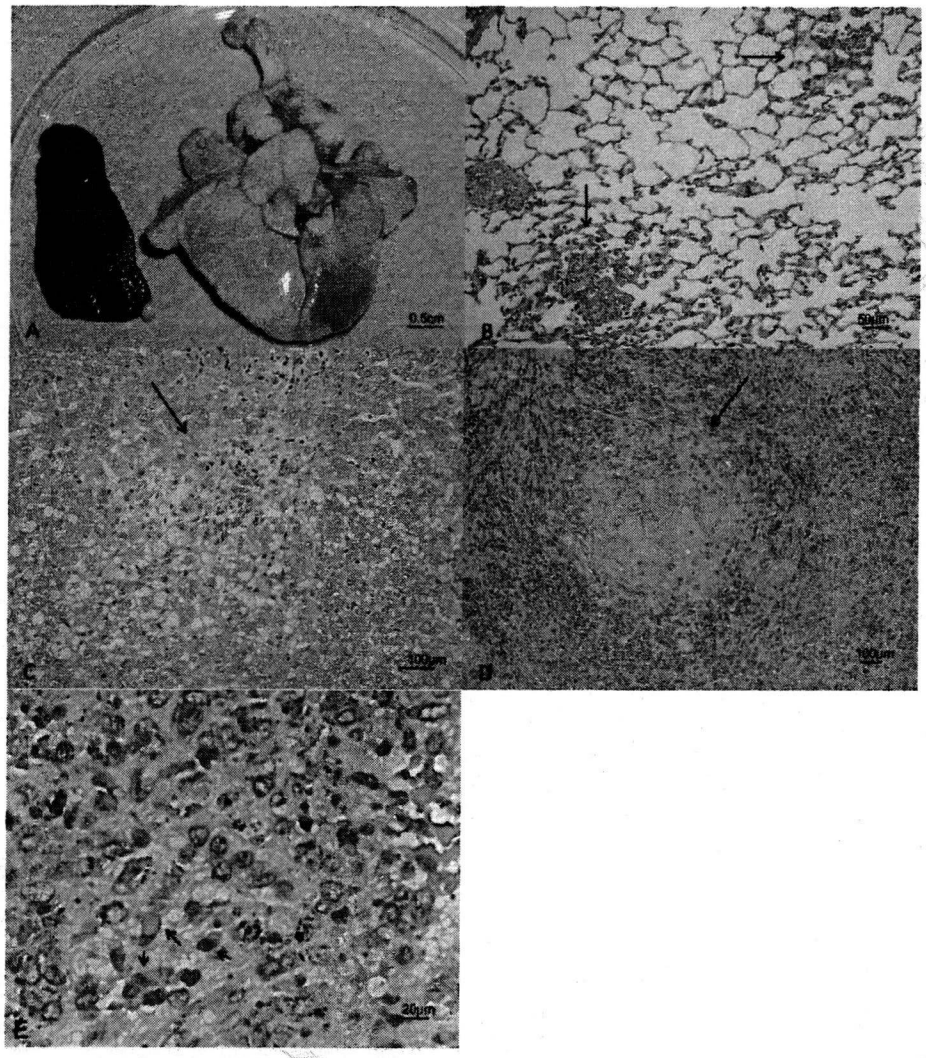

Fig. 1. Pathology of lung, spleen, and liver tissues from guinea pigs infected with GFP-H37Rv. A, Macroscopy of infected guinea pig organs; B, Lung tissue; C, Liver tissue; D, Spleen tissue; E, Epithelioid macrophages (→) immunostained with anti-BCG polyclonal antibody and counter-stained with hematoxylin. Arrow (→) indicates the microgranuloma in B, C, and D. Hematoxylin eosin stain × 100.

Results

Infection of guinea pigs with GFP-H37Rv, and macroscopic and microscopic pathology

To begin characterizing the infection caused by the GFP-H37Rv strain, the guinea pigs were inoculated subcutaneously with very low doses of tubercle bacilli (100 or 1,000 CFU) and then followed up for 10 months. First, we monitored for external clinical changes related to tuberculosis in guinea pigs (lethargy, scuffed fur, foot-dragging walk, weight loss). Over the 10-month period, the guinea pigs inoculated with 100 CFU GFP-H37Rv showed none of the above-mentioned signs except gradual increase of body weight and no changes in overall behavior. The guinea pigs inoculated with 1,000 CFU GFP-H37Rv showed no scuffing of the fur, foot-dragging walk, or lethargy for the first 8 months, but thereafter a foot-dragging walk appeared. No loss of body weight was observed in this group; all 10 infected guinea pigs (1,000 CFU inoculation) steadily gained weight throughout the experiment, and no deaths occurred.

There were no macroscopic lesions suggestive of tuberculosis at 10 months in 100 CFU-inoculated group (Fig. 1A). However, histopathological examination showed microgranulomas in the lungs in 100 CFU-inoculated group, the liver parenchyma, and the lymph follicles of the spleen (Fig. 1B-D). Only one tubercle bacillus was found in one lung tissue section stained by Ziehl-Neelsen stain for acid-fast bacilli. Immunohistochemistry using anti-BCG polyclonal antibody demonstrated BCG antigens in the epithelioid macrophages that constituted the microgranulomas (Fig. 1E).

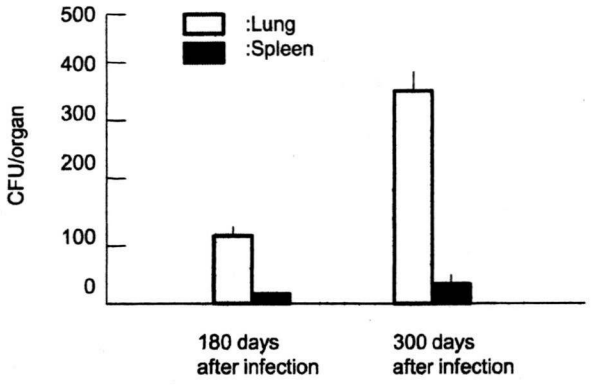

Fig. 2. Persistence of viable GFP-H37Rv strain in the tissues of infected guinea pigs. CFU counts were made on lung and spleen tissues 180 and 300 days after infection (three per group).

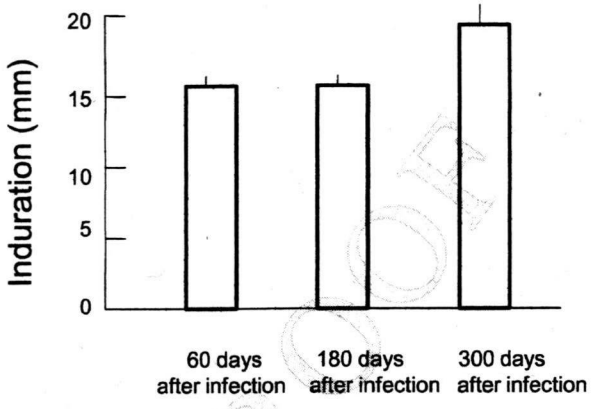

Fig. 3. PPD skin testing of guinea pigs infected with GFP-H37Rv.
Skin tests were performed 60, 180, and 300 days after infection (three per group), and the diameter of the induration was measured in mm.

Burden of mycobacteria in guinea pig tissues after subcutaneous infection with GFP-H37Rv

To confirm that infection of guinea pigs with the GFP-H37Rv resulted in latent infection, 180 and 300 days after infection CFU counts were made in the pulmonary and splenic tissues of guinea pigs that had been inoculated with 100 CFU GFP-H37Rv. At 180 days after infection the pulmonary CFU was 121 ± 10, and 300 days after infection it was 360 ± 15 (Fig. 2). The splenic CFU counts 180 and 300 days after infection were 10 ± 1 and 25 ± 2, respectively.

PPD skin testing

We used the tuberculin purified protein derivative (PPD) skin test, because it is used worldwide as an adjunctive test for the diagnosis of both latent and active tuberculosis. All infected guinea pigs were strongly positive in all PPD tests, which were performed at 60 days (16.3 ± 1.1 mm diameter), 180 (16.7 ± 1.3 mm), and 300 days (19.7 ± 1.4 mm) after infection (Fig. 3). No induration reaction was recognized in the skin of uninfected control guinea pigs ($n = 5$).

Photon imaging of organs from guinea pigs

To localize the lesions suggestive of the presence of GFP-H37Rv, the major organs were serially cut to a thickness of 5 mm and subjected to photon imaging. Strong red signals of varying intensities were recognized in the serially cut lung and liver tissues from infected guinea pigs (Fig. 4A and 4B). Strong red signals were also detected in the spleen. The locations of the strong signals corresponded to the granulomas (proliferative inflammation) found on histopathological examination (see Fig. 1).

Real-time PCR analysis of infected pulmonary tissues

Data obtained by real-time PCR analysis of infected pulmonary tissues were expressed as relative intensities. In the lung tissues of uninfected guinea pigs, expression levels of IFN-γ, TNF-α, IL-10, IL-12, and iNOS mRNAs were very low (< 0.1 as relative intensity). At 180 days after infection, there were no statistically significant differences in mRNA expression between uninfected and infected guinea pigs (Table 1). At 300 days after infection the intensities were minimal, but significant differences in IFN-γ, TNF-α, IL-12, and iNOS mRNA expression were recognized between uninfected and infected guinea pigs ($P < 0.01$).

Discussion

In this study we have reported the successful establishment of latent *M. tuberculosis* infection in guinea pigs. In human tuberculosis, exogenous reinfection and reactivation of *M. tuberculosis* are major problems that require resolution, but in order to do so, the pathogenesis of latent human tuberculosis needs to be clarified. Because we did not have an animal model suitable for the investigation of latent tuberculosis, it was of great importance to develop one in order to study the pathogenesis and molecular mechanisms of latent infection.

Several murine models of latent infection have already been reported (McCune et al. 1956; Orme 1987; Phyu et al. 1998). In a model known as the Cornell model, mice are inoculated intravenously with viable tubercle bacilli and the resulting infection is treated for 12 weeks with anti-mycobacterial drugs. From this time point on, no tubercle bacilli can be cultured from the organs of these animals for several months. Administration of cortisone 2 to 3 months after interruption of the antibiotic therapy reverses this condition, and tubercle bacilli can then be cultured from lungs and spleens of more than 50% of the animals. The Cornell model is therefore not so highly reproducible and has no standardized protocol for establishment of latency. Although variant Cornell murine models have been proposed, their reproducibility is still low and many parameters (inoculating dose, infection period, antibiotics, and duration

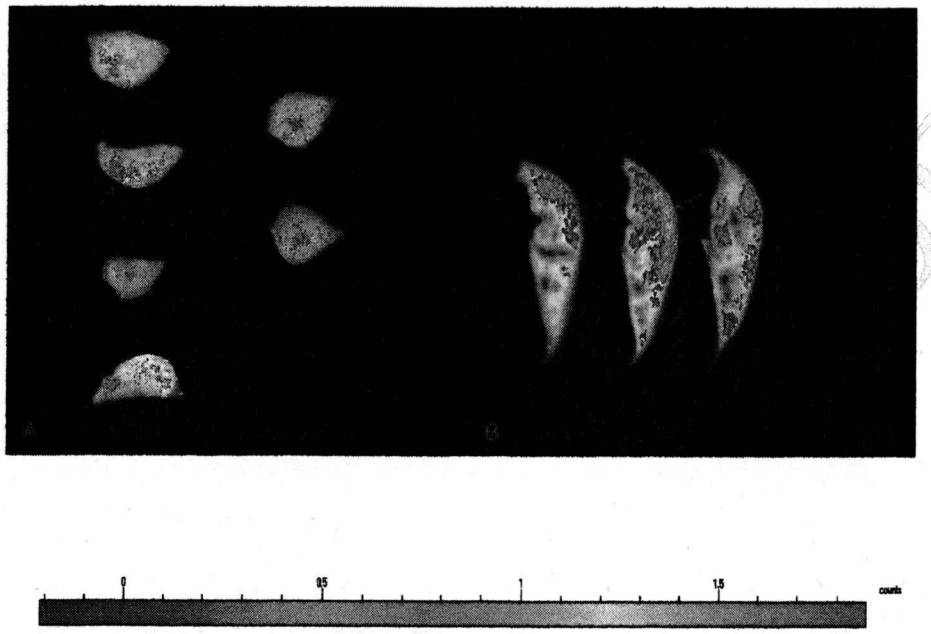

Fig. 4. Visualizing granulomas in the lung and liver of infected guinea pigs.
Small pulmonary (A) and liver (B) granulomas were visualized by photon imaging. Granulomatous lesions are visible as strong red signals (→).

Table 1. Expression profiles of IFN-γ, TNF-α, IL-10, IL-12, and iNOS mRNAs in the lungs of infected guinea pigs.

	IFN-γ*	TNF-α	IL-10	IL-12	iNOS
180 days after infection	1.12	1.20	0.95	1.05	1.17
300 days after infection	1.74+	1.89+	1.02	1.79+	2.09+

The guinea pigs were inoculated with 100 CFU GFP-H37Rv. *In the lung tissues of uninfected guinea pigs, expression levels of IFN-γ, TNF-α, IL-10, IL-12, and iNOS mRNA were very low (< 0.1 as relative intensity).

+Statistically significant ($P < 0.01$).

of treatment) are involved in the induction of latency (Scanga et al. 1999).

In low-dose murine models, mice are aerogenically or intraperitoneally infected with a low dose of *M. tuberculosis*. The quiescent phase of the infection is maintained for a relatively long time, after which the infection begins to reactivate and the mice succumb to tuberculosis (Orme 1987). This low-dose murine model has the important advantage of tracing natural latency in the sense that it relies solely on the host immune response for control of the infection. However, it has the disadvantage of a high bacillary burden, unlike that found in human latent *M. tuberculosis* infection.

A guinea pig model of *M. tuberculosis* latent or dormant infection was therefore proposed recently (Kashino et al. 2008). This model employs a streptomycin-auxotrophic mutant of *M. tuberculosis* (*M. tuberculosis* 18b) and streptomycin. However, this model is not still reproducible, because 10^7 CFU of *M. tuberculosis* 18b are injected intravenously and the guinea pigs are then inoculated with streptomycin for 3 months. To overcome this difficulty, we created a low-dose model by injecting guinea pigs subcutaneously with 100 or 1,000 CFU GFP-H37Rv. Ten months later, no mycobacterial lesions were observed macroscopically, but all of the tuberculin skin tests conducted during the follow-up period gave positive results. However, the lymphocytes from the hilar lymph nodes of the latent guinea pig tuberculosis did not respond to Ag85A peptides in vitro (data not shown). It was not easy to detect granulomas histopathologically, but use of a photon imaging technique clearly localized the granulomatous lesions in the organs. The 1,000-CFU subcutaneous model was not suitable for latent infection because the tubercle bacilli were reactivated 10 months later and many granulomatous lesions were recognizable in the major organs. Conversely, the 100-CFU model was favorable in that only microgranulomas were observed histologically. To date we have followed up the 100-CFU group for more than 1 year; the guinea pigs are all still alive and their tuberculin skin tests still give positive results.

To shed light on the molecular mechanisms of latent tuberculosis, we examined the expression of cytokine and iNOS mRNAs. At 180 days after infection there were no significant differences in mRNA expression between uninfected and latently infected guinea pigs, but significant changes in expression of IFN-γ, TNF-α, IL-12, and iNOS mRNAs were recognized between uninfected and latently infected animals at 300 days after infection. These results indicate that the immune network (Th2 cytokines and the cytokines related to Th2 cells) was stimulated minimally but effectively in latent infection.

Our animal model should provide useful clues for studying the pathology of adult latent tuberculosis. Humans and rabbits infected with *M. tuberculosis* develop cavities in the lungs, whereas guinea pigs do not (Dannenberg 2006). After reactivation of latent infection or exogenous reinfection with *M. tuberculosis*, caseous lesions and cavities may develop. Further study will be required to elucidate the mechanisms involved. Our model may also be of help for studying new tuberculosis vaccines and drugs for latent tuberculosis. As mentioned above, it is difficult to detect microgranulomas, but they were clearly detectable with a high-sensitivity photon imager. If a drug or vaccine being tested were effective in latent tuberculosis, then no fluorescent signals would be detected. Our model is therefore an attractive alternative for use in the development of anti-tuberculosis vaccines in the context of presensitization of animals.

In summary, we have established a guinea pig model of latent tuberculosis. Our guinea pig model can be used widely for studies of the immunology, molecular biology, and chemotherapy of latent tuberculosis.

Acknowledgments

This project was supported in part by a grant-in-aid from the Ministry of Health, Labor, and Welfare, Japan.

References

Dannenberg, A.M. (2006) Pathogenesis of human pulmonary tuberculosis. Insights from the rabbit model. ASM press, Washington, D.C.

Hashimoto, T. (1955) Experimental studies on the mechanism of infection and immunity in tuberculosis from the analytical standpoint of streptomycin-dependent tubercle bacilli. 1. Isolation and biological characteristics of a streptomycin-dependent mutant and effect of streptomycin administration on its pathogenicity in guinea pigs. *Kekkaku*, **30**, 4-8 (in Japanese).

Hsu, S.M., Raine, L. & Fanger, H. (1981) Use of avidin-biotin-peroxidase complex (ABC) in immunoperoxidase techiniques: a comparison between ABC and unlabeled antibody (PAP) procedures. *J. Histochem. Cytochem.*, **29**, 577-580.

Hyoudou, K., Nishikawa, M., Kobayashi, Y., Kuramoto, Y., Yamashita, F. & Hashida, M. (2007) Analysis of in vivo nuclear factor-κB activation during liver inflammation in mice: Prevention by catalase delivery. *Mol. Pharmacol.*, **71**, 446-453.

Kashino, S.S., Napolitano, D.R., Skobe, Z. & Campos-Neto, A. (2008) Guinea pig model of Mycobacterium tuberculosis latent/dormant infection. *Microbes Infect.*, **10**, 1469-1476.

Lurie, M.B. (1950) Native and acquired resistance to tuberculosis. *Am. J. Med.*, **9**, 591-610.

McCune, R.M., McDermott, W. & Tompsett, R. (1956) The fate of Mycobacterium tuberculosis in mouse tissues as determined by the microbial enumeration techniques. II. The conversion of tuberculous infection to the latent state by the administration of pyrazinamide and a companion drug. *J. Exp. Med.*, **104**, 763-802.

Medlar, E.M. (1950) Pathogenetic concepts of tuberculosis. *Am. J. Med.*, **9**, 611-622.

Orme, I.M. (1987) A mouse model of the recrudescence of latent tuberculosis in the elderly. *Am. Rev. Respir. Dis.*, **137**, 716-718.

Phyu, S., Mustafa, T., Hofstad, T., Nilsen, R., Fosse, R. & Bjune, G. (1998) A mouse model for latent tuberculosis. *Scand. J. Infect. Dis.*, **30**, 59-68.

Scanga, C.A., Mohan, V.P., Joseph, H., Yu, K., Chan, J. & Flynn, J.L. (1999) Reactivation of latent tuberculosis: variations on the Cornell murine model. *Infect. Immun.*, **67**, 4531-4538.

Shi, R., Zhnag, J., Li, C., Kazumi, Y. & Sugawara, I. (2007) Detection of streptomycin resistance in *Mycobacterium tuberculosis* clinical isolates from China as determined by denaturing HPLC analysis and DNA sequencing. *Microbes Infect.*, **9**, 1538-1544.

Sugawara, I., Yamada, H., Kazumi, Y., Doi, N., Otomo, K., Aoki, T., Mizuno, S., Udagawa, T., Tagawa, Y. & Iwakura, Y. (1998) Induction of granulomas in interferon-γ gene-disrupted mice by avirulent but not by virulent strains of *Mycobacterium tuberculosis*. *J. Med. Microbiol.*, **47**, 871-877.

Sugawara, I., Yamada, H. & Mizuno, S. (2004) Pulmonary tuberculosis in spontaneously diabetic Goto Kakizaki rats. *Tohoku J. Exp. Med.*, **204**, 135-145.

Sugawara, I., Yamada, H. & Mizuno, S. (2006) Nude rat (F344/N-rnu) tuberculosis. *Cell. Microbiol.*, **8**, 661-667.

Sugawara, I., Mizuno, S., Tatsumi, T. & Taniyama, T. (2006) Imaging of pulmonary granulomas using a photon imager. *Jpn. J. Infect. Dis.*, **59**, 332-333.

Yamada, H., Mizuno, S., Reza-Gholizadeh, M. & Sugawara, I. (2001) Relative importance of NF-κB p50 in mycobacterial infection. *Infect. Immun.*, **69**, 7100-7105.

Yamada, H., Udagawa, T., Mizuno, S., Hiramatsu, K. & Sugawara, I. (2005) Newly designed primer sets available for evaluating various cytokines and iNOS mRNA expression in guinea pig lung tissues by RT-PCR. *Exp. Anim.*, **54**, 163-172.

Yamada, H., Mizuno, S., Ross, A.C. & Sugawara, I. (2007) Retinoic acid therapy attenuates the severity of tuberculosis while altering lymphocyte and macrophage numbers and cytokine expression in rats infected with Mycobacterium tuberculosis. *J. Nutr.*, **137**, 2696-2700.

Jpn. J. Infect. Dis., 62, 390-391, 2009

Short Communication

Tuberculosis Complicated by Diabetes Mellitus at Shanghai Pulmonary Hospital, China

Qing Zhang, Heping Xiao, and Isamu Sugawara[1]*

Department of Tuberculosis, Shanghai Pulmonary Hospital, Shanghai, China; and
[1]The Research Institute of Tuberculosis, Tokyo 204-0022, Japan

(Received June 8, 2009. Accepted July 17, 2009)

SUMMARY: An association between diabetes mellitus (DM) and tuberculosis (TB) has been implied for a long time. We previously reported that KDP type 1 diabetic rats and GK type 2 diabetic rats are highly susceptible to *Mycobacterium tuberculosis* infection. As a next step, we conducted a retrospective analysis of 2,141 patients with pulmonary TB newly diagnosed during the period from 2008 to 2009 to evaluate the influence of DM on the drug response rate and the long-term relapse rate of TB. There were 203 DM patients with TB (type 1 DM, 7 [3.4%]; type 2 DM, 196 [96.6%]). The TB relapse rate (2 years after discharge) was higher in DM patients than in non-diabetic patients (20% versus 5.3%). The frequency of multidrug-resistant-TB among DM patients with TB was higher than that among TB patients (17.7% versus 8.4%, $P < 0.01$). These results suggest that the period of TB treatment should be prolonged, and that in the meantime the blood glucose level should be maintained within a reference value range.

Diabetes mellitus (DM) is a high-risk factor for tuberculosis (TB). An association between diabetes and TB has been implied for centuries. In the late 17th century, Morton recognized a link between diabetes and TB (1). Since then, a body of clinicoepidemiological data has been accumulated (2-7). However, there is no definitive evidence of an association between DM and TB. Patients with DM have been noted to have impaired granulocyte chemotaxis, phagocytosis, bactericidal activity and superoxide production (8,9). In order to obtain conclusive evidence of the link between DM and TB, we have employed two kinds of rat diabetes models, the Komeda diabetes-prone (KDP) type 1 rat model and the Goto-Kakizaki (GK) type 2 rat model, and have reported that both type 1 and type 2 diabetic rats are highly susceptible to *Mycobacterial tuberculosis* (10,11). Although there are a few reports on the association between TB and DM in Asia (7,12,13), no such report has come from China. Therefore, we focused on TB patients with DM in Shanghai, China. A total of 2,141 TB patients were hospitalized between April 2008 and March 2009, of whom 1,464 (68.4%) were smear- and culture-positive, and 20.2% were smear-negative and culture-positive. The male to female ratio was 3.2:1. All were farmers, salaried persons or unemployed, with an average age of 42.7 years. This project was approved by the ethics committee of Shanghai Pulmonary Hospital, China.

Among these TB patients, 203 (9.5%) were complicated by DM (type 1, 7; type 2, 196). Of these, 114 patients were smear- and culture-positive and 47 were smear-negative and culture-positive. The blood glucose range of these patients was 200-700 mg/dl. After the DM patients had been hospitalized for 2 to 4 weeks, those with type 1 DM were treated by subcutaneous injection of recombinant insulin, and those with type 2 DM received oral medication including metformin hydrochloride and gliclazide. Thereafter, they received standardized regimens consisting of isoniazid, rifampicin, pyrazinamide, ethambuthol or streptomycin. We then examined the drug susceptibility of *M. tuberculosis* isolates cultured from the TB patients with DM by the proportional method (14). As shown in Table 1, 36 (17.7%) of the patients with DM had multidrug-resistant (MDR)-TB, the proportion being significantly higher than that of non-diabetics with TB (9.3%) ($P < 0.01$). Furthermore, the proportion of MDR-TB patients was much higher in the group with poorly controlled DM (32 versus 4). Of 167 patients who had received standardized chemotherapy, 20 (12.0%) relapsed within 2 years after being discharged from the hospital. There are several reasons that the incidence of MDR-TB and the relapse rate are higher in patients with DM than in non-diabetics. First, the DM patients have moderate to severe TB, and it takes longer period to treat them sufficiently with chemotherapy. Their drug compliance is often poor, and they suffer adverse reactions more frequently. They take anti-TB drugs irregularly. Second, some patients cannot pay for their medical expenses, and so their chemotherapy has to be discontinued for short periods of time until they earn enough money to restart the chemotherapy. Third, some patients do not take anti-DM drugs regularly, and their blood glucose levels are not well controlled, until eventually their TB becomes refractory. Lastly, these DM patients may be reinfected with new MDR-TB strains due to their lowered immunity.

Table 1. Drug sensitivity of tubercle bacilli cultured from TB patients with DM

	Drug-susceptible	MDR[1)]	Total
Diabetics ($n = 203$)[2)]	82.3%	36 (17.7%)	100%
FBS ≧ 200 mg/dl		32 (15.7%)	
126 ≦ FBS ≦ 199		4 (2.0%)	
Non-diabetics ($n = 1,938$)	90.7%	9.3%	100%

[1)]: $P < 0.01$.
[2)]: The detailed profiles of 203 diabetics and 1,938 non-diabetics are as follows: 67 (FBS ≧ 200 mg/dl) (51-78 years old, man:woman = 5.5:1), 136 (126 ≦ FBS ≦ 199) (30-82 years old, man:woman = 5.5:1), and 1,938 (FBS≦125) (2-96 years old, man:woman = 3:1).
MDR, multidrug-resistant; FBS, fasting blood sugar (mg/dl).

*Corresponding author: Mailing address: The Research Institute of Tuberculosis, 3-1-24 Matsuyama, Kiyose, Tokyo 204-0022, Japan. Tel: +81-42-493-5075, E-mail: sugawara@jata.or.jp

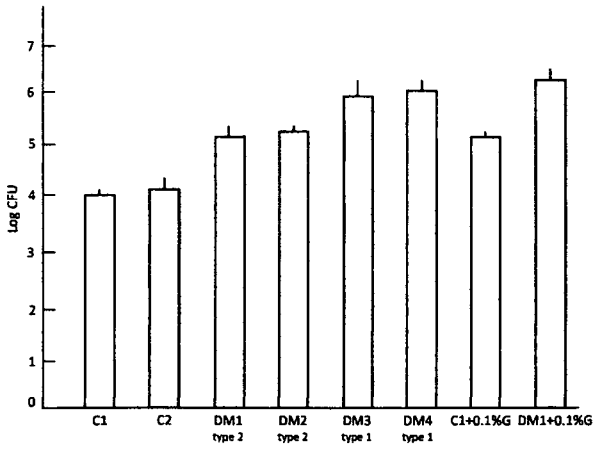

Fig. 1. The effect of serum from DM patients on growth of *M. tuberculosis* H37Rv. C, healthy volunteer; DM, diabetes mellitus; G, glucose.

There have been two reports of pulmonary TB complicated by DM in Japan (12,13). Kameda et al. analyzed 116 TB patients with DM among 644 TB patients. MDR-TB patients with DM accounted for 6.0% of the total, which was a significantly lower proportion than that in our present series. Their relapse rate within 30 months after discharge was 10.3%, which was not significantly different from the result in our series. Wada et al. also reported 54 TB patients with DM among 620 patients with TB, and the relapse rate within 24 months after discharge was 11.1%, compared with 1.3% in non-diabetics. This difference was statistically significant ($P < 0.01$). Thus, it is worthwhile to examine the TB relapse rate in diabetics on the basis of large samples.

We have recently reported that 0.1% glucose increased mycobacterial growth in vitro and that insulin treatment resulted in a significant reduction of tubercle bacilli in infected KDP rats (13). Therefore, it is useful to examine the effects of serum samples from DM patients on mycobacterial growth in vitro. We collected two serum samples from healthy subjects (C1 and C2), two samples from type 2 DM patients (DM1 and DM2) and two samples from type 1 DM patients (DM3 and DM4). Blood glucose levels and immunoreactive insulin (IRI) levels in DM1, DM2, DM3 and DM4 were 520 mg/dl and 5 μU/ml, 660 mg/dl and 5 μU/ml, 610 mg/dl and <1 μU/ml, and 705 mg/dl and <1 μU/ml, respectively. The reference value ranges of fasting blood glucose and IRI were 100-125 mg/dl and 5-15 μU/ml, respectively, in this hospital. The patients' serum (0.5 ml each) was added to 0.5 ml of 7H9 liquid medium and cultured in the presence of *M. tuberculosis* H37Rv (1,000 CFU) for 1 week. Thereafter, serially diluted samples were cultured on 1% Ogawa solid agar slants in triplicate, and the colonies that appeared were counted 4 weeks later. In some experiments, 0.1% glucose was added to C1 and DM1 serum samples. As shown in Fig. 1, the growth of tubercle bacilli was facilitated in the patients' sera. Moreover, the sera from type 1 DM patients enhanced mycobacterial growth significantly ($P < 0.01$). When 0.1% glucose was added to C1 and DM1 serum samples, the growth of tubercle bacilli was better facilitated ($P < 0.01$). Although the sample numbers were small, the results suggested that glucose stimulates mycobacterial growth, whereas insulin reduces mycobacterial colonies.

We then conducted a retrospective analysis of 2,141 patients with pulmonary TB newly diagnosed during the period from 2008 to 2009 to evaluate the influence of DM (203 cases) on the drug response rate and the long-term TB relapse rate. The cases of TB complicated by DM showed a poor prognosis if relapse occurred within 2 years. Thus, it appears that a longer treatment period is required for TB patients with DM. At the same time, as there were more MDR-TB patients with DM in this series, there is a need to devise a new chemotherapy regimen to achieve a more effective treatment.

REFERENCES

1. Morton, R. (1694): *Phthisiologia*. Smith and Welford, London, England.
2. Banyai, A.L. (1931): Diabetes and pulmonary tuberculosis. Am. Rev. Tuberc., 24, 650-667.
3. Root, H.F. (1934): The association of diabetes and tuberculosis. N. Engl. J. Med., 210, 1-13.
4. Boucot, K., Dillon, E., Cooper, D., et al. (1952): Tuberculosis and diabetics. Am. Rev. Tuberc., 65 (Suppl. 1), 1-50.
5. Mugusi, F., Swai, A.B.M., Alberti, K.G.M.M., et al. (1990): Increased prevalence of diabetes mellitus in patients with pulmonary tuberculosis in Tanzania. Tubercle, 71, 271-276.
6. Koziel, H. and Koziel, M.J. (1995): Pulmonary complications of diabetes mellitus: pneumonia. Infect. Dis. Clin. North Am., 9, 65-96.
7. Kim, S.J., Hong, Y.P., Lew, W.J., et al. (1995): Incidence of pulmonary tuberculosis among diabetics. Tuber. Lung Dis., 76, 529-533.
8. Geisler, C., Almdad, T., Bennedsen, J., et al. (1982): Monocyte functions in diabetes mellitus. Acta Pathol. Microbiol. Immunol. Scand., 90, 33-37.
9. Glass, E.J., Stewart, J., Matthews, D.M., et al. (1987): Impairment of monocyte 'lectin-like' receptor activity in type I (insulin dependent) diabetic patients. Diabetologia, 30, 228-231.
10. Sugawara, I., Yamada, H. and Mizuno, S. (2004): Pulmonary tuberculosis in spontaneously diabetic Goto Kakizaki rats. Tohoku J. Exp. Med., 204, 135-145.
11. Sugawara, I. and Mizuno, S. (2008): Higher susceptibility of type 1 diabetic rats to *Mycobacterium tuberculosis* infection. Tohoku J. Exp. Med., 216, 363-370.
12. Kameda, K., Kawabata, S. and Masuda, N. (1990): Follow-up study of short course chemotherapy for pulmonary tuberculosis complicated with diabetes mellitus. Kekkaku, 65, 791-803 (text in Japanese).
13. Wada, M., Yoshiyama, T., Ogata, H., et al. (1999): Six-months chemotherapy (2HRZS or E/4HRE) of new cases of pulmonary tuberculosis—six years experiences on its effectiveness, toxicity, and acceptability. Kekkaku, 74, 353-360 (text in Japanese).
14. Shi, R., Zhang, J., li, C., et al. (2007): Detection of streptomycin resistance in *Mycobacterium tuberculosis* clinical isolates from China as determined by denaturing HPLC analysis and DNA sequencing. Microbes Infect., 9, 1538-1544.

Indian Journal of Experimental Biology
Vol. 47, June 2009, pp. 520-522

Cross-resistance of *Mycobacterium tuberculosis* isolates among streptomycin, kanamycin and amikacin

I Sugawara[1]*, J Zhang[2] & C Li[2]

[1]Mycobacterial Reference Center, The Research Institute of Tuberculosis, 3-1-24 Matsuyama, Kiyose, Tokyo 204-0022, Japan

[2]Beijing Tuberculosis and Lung Tumor Research Institute, Beijing, China

Received 8 December 2008

Seventy-four streptomycin (SM)-resistant *M. tuberculosis* clinical isolates were subjected to cross-resistance drug testing against two major aminoglycosides, kanamycin (KM) and amikacin (AMK). Among them, 15 clinical isolates (20.3%) were resistant to both KM and AMK. Fifteen (80%) of 19 KM-resistant isolates were AMK-resistant. Fifteen SM, KM, and AMK resistant isolates harbored *rrs* mutation, but only two had *rrs* and *rpsL* double mutations. Low-level SM resistance was associated with *rpsL* mutation, whereas high-level SM resistance was linked to *rrs* mutation.

Keywords: Amikacin, Cross-resistance, Kanamycin, MDR-TB, Streptomycin

Streptomycin (SM) is one of the aminoglycosides and is used as a first-line anti-tuberculosis (anti-TB) drug. Its structure is o-2-deoxy-2-(methylamino)-α-L-glucopyranosyl-(1→2)-o-5-deoxy-3-C-formyl-α-L-lyxofuranosyl-(1→4)-N,N'-bis(aminoiminomethyl)-D-streptamine. Earlier in a study, we used 115 streptomycin (SM)-resistant clinical isolates from Beijing, China, of which 85.2% harbored *rpsL* or *rrs* mutation, while *rpsL* mutation (76.5%) dominated among the isolates[1]. Among them, 45 clinical isolates were resistant to SM at more than 100 μg/mL and regarded as high-level SM-resistant. These 115 SM-resistant clinical isolates were collected from local farmers (treated previously with several anti-TB drugs) from all over China and sent to Beijing Tuberculosis and Lung Tumor Research Institute for further survey. There are reports that kanamycin (KM) and/or amikacin (AMK) are used as second-line anti-TB drugs for patients with MDR-TB and KM and AMK kill SM-resistant isolates[2].

KM and AMK are aminoglycosides with the structures o-3-amino-3-deoxy-α-D-glucopyranosyl-(1→6)-o-[6-amino-6-deoxy-α-D-glucopyranosyl-(1→4)]-2-deoxy-D-streptamine and o-3-amino-3-deoxy-α-D-glucopyranosyl-(1→6)-o-[6-amino-6-deoxy-α-D-glucopyranosyl-[1→4]]-N1-(4-amino-2-hydroxy-1-oxobutyl)-2-deoxy-D-streptamine, respectively. It indicates that SM, KM and AMK have similar structures. Moreover, KM and AMK are used as second-line anti-TB drugs for patients with MDR-TB, but there is no report on cross-resistance among SM, KM and AMK based on large clinical samples[3]. In view of this, the present study was undertaken to elucidate the cross-resistance among SM, KM, and AMK.

Seventy-four streptomycin (SM)-resistant and 11 SM-sensitive clinical isolates of *M. tuberculosis* from China were considered for the study. The 74 patients with SM-resistant TB had been treated with several anti-TB drugs, but had no previous history of KM and AMK treatment. There were no mono-resistant SM clinical isolates. Several isolates did not grow well and hence, were omitted from this study. Minimum inhibitory concentrations (MICs) of SM, KM, and AMK were detected by absolute concentration method in L-J medium at 1, 2, 5, 10, 20, 40, 80, 100, 200, 400, 800 and 1,000 μg/mL (Ref. 1). Isolates with a MIC exceeding 10 μg/mL are defined as SM-resistant[4,5]. However, for KM and AMK resistance, MIC was 20 μg/mL (Refs 4, 6).

Forty-five isolates (61%) were resistant to SM at more than 100 μg/mL and referred to as high-level SM resistance (Fig. 1). Twelve isolates had a MIC of less than 40 μg/mL. On the other hand, there were 19 KM-resistant isolates, and 15 of them were resistant to concentrations exceeding 100 μg/mL. There were 15 AMK-resistant isolates, of which 9 were resistant at more than 100 μg/mL of concentration. There were 15 isolates resistant to both KM and AMK, and 9 (60%) of them were resistant to concentrations exceeding 100 μg/mL (Table 1).

*Correspondent author
Telephone: +81 (42) 493 5075; Fax: +81 (42) 492 4600
E-mail: sugawara@jata.or.jp

It has been considered worth to examine these 15 SM, KM and AMK resistant clinical isolates genetically in terms of *rpsL* and *rrs* mutations[6,7]. We utilized a denaturing HPLC (DHPLC) system to detect point mutation of target genes as reported previously[1,8]. All the isolates displayed *rrs* mutation and three of them had *rpsL* mutation (Table 2)[9]. The most common *rrs* mutation (^{513}A→C) was found in 7 isolates. Interestingly, high-level SM resistance was closely associated with both KM and AMK resistance [15/45 (33%)]. The target genes of SM were *rpsL* and *rrs*, while a target gene of KM and AMK was *rrs*. As all SM-resistant clinical isolates possessed *rrs* mutation, they were also resistant to KM and AMK. Among 11 SM-sensitive isolates, only two were resistant to KM and AMK. Thus, there were cases that KM or AMK could not be used as a second-line drug for MDR-TB patients with high-level SM resistance.

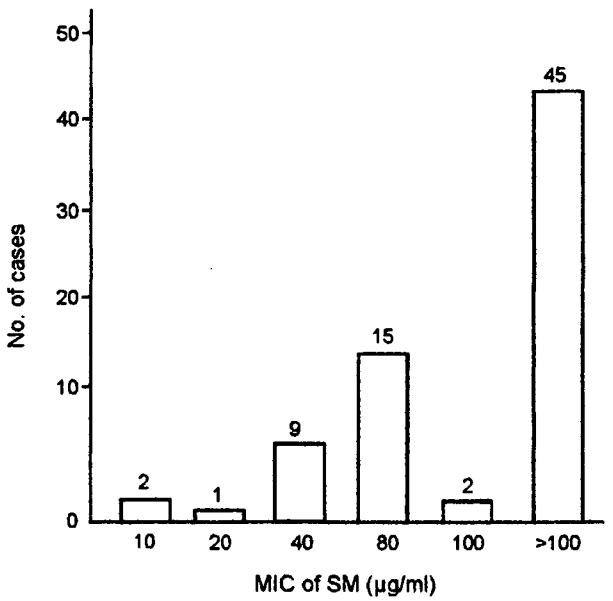

Fig. 1—Frequency of 74 SM-resistant clinical isolates at different MIC.

Table 1—Cross-resistance of 74 SM-resistant *M. tuberculosis* clinical isolates to KM and/or AMK

Drug resistance	No. of clinical isolates
Resistance to SM	74
High-level SM resistance	45 (61%)
Resistance to KM	19 (25.75%)
High-level KM resistance	15
Resistance to AMK	15 (20.3%)
High-level AMK resistance	9
Resistance to KM & AMK	15 (20.3%)
High-level KM & AMK resistance	9

SM- streptomycin; KM- kanamycin; and AMK- amikacin

Table 2—*rpsL* and *rrs* mutation of 15 SM-, KM- and AMK-resistant *M. tuberculosis* clinical isolates

Clinical isolate No.	*rpsL* mutation	*rrs* mutation
1	codon 43 (AAG→AGG)	^{513}A→C
2	none	645deletion
3	none	^{513A}→C
4	none	^{513}A→C
5	none	^{513}A→C
6	none	^{513}A→C
7	none	^{513}A→C
8	none	^{516}C→T
9	none	^{464}A→C
10	none	^{906}A→C
11	codon 43 (AAG→AGG)	^{1400}A→G
12	codon 43 (AAG→AGG)	^{1401}C→T
13	none	^{1401}C→T
14	none	^{513}A→C
15	none	^{513}A→C

SM- streptomycin; KM- kanamycin; and AMK- amikacin

In the present study, it was found that MDR-TB cases were not only confined to China, but also found three SM-, KM- and AMK-resistant cases in Osaka, Japan. There were not many such cases in Japan (Personal communication with Dr. K. Tsuyuguchi, Japan).

In conclusion, it seems that there are few reports on no cross-resistance between SM and KM or SM and AMK, as long as we searched in the literature[2,5]. It is concluded that high-level SM resistance is closely linked to mutation of *rrs*, which is a target gene of KM and AMK, whereas low-level SM is linked to *rpsL* mutation.

References

1 Shi R, Zhang J, Li C, Kazumi Y & Sugawara I, Detection of streptomycin resistance in *Mycobacterium tuberculosis* clinical isolates from China as deteremined by denaturing HPLC analysis and DNA sequencing. *Microbes Infect*, 9 (2007) 1538.

2 Tsukamura M & Mizuno S, Cross-resistance relationships among the aminoglycoside antibiotics in *Mycobacterium tuberculosis*, *J Gen Microbiol*, 88 (1975) 269.

3 Alangaden G J, Kreiswirth B N, Aouad A, Khetarpal M, Igno

F R, Moghazeh S L & Manavathu E K, Mechanism of resistance to amikacin and kanamycin in *Mycobacterium tuberculosis*. *Antimicrob Agents Chemother*, 42 (1998) 1295.

4 Allen B W, Mitchison D A, Chan Y C, Yew W W, Allan W G L & Girling D J, Amikacin in the treatment of pulmonary tuberculosis. *Tubercle*, 64 (1983) 111.

5 Katsukawa C, Tamaru A, Miyata Y, Abe C, Makino M & Suzuki Y, Characterization of the *rpsL* and *rrs* genes of streptomycin-resistant clinical isolates of *Mtcobacterium tuberculosis* in Japan. *J Appl Microbiol*, 83 (1997) 634.

6 *Guidelines for Mycobacterium tuberculosis examination, 2007* (Mycobacterial Methods Evaluation Committee of Japanese Society for Tuberculosis, Kekkaku Yobokai, Tokyo) 2007.

7 Finken M P, Kirschner A, Meier A, Wrede E & Böttger E C, Molecular basis of streptomycin resistance in *Mycobacterium tuberculosis* alterations of the ribosomal protein S12 gene and point mutations within a functional 16S ribosomal RNA pseudoknot. *Mol Microbiol*, 9 (1993) 1239.

8 Shi R, Zhang J, Otomo K, Zhang G & Sugawara I, Lack of correlation between *embB* mutation and ethambutol MIC in *Mycobacterium tuberculosis* clinical isolates from China. *Antimicrob Agents Chemother*, 51 (2007) 4515.

9 Nair J, Rouse D A, Bai G H & Morris S L, The *rpsL* gene and streptomycin resistance in single and multiple drug-resistant strains of *Mycobacterium tuberculosis*, *Mol Microbiol*, 10 (1993) 521.

INFECTION AND IMMUNITY, Sept. 2009, p. 3992–4001 Vol. 77, No. 9
0019-9567/09/$08.00+0 doi:10.1128/IAI.00015-09

The RD1 Locus in the *Mycobacterium tuberculosis* Genome Contributes to Activation of Caspase-1 via Induction of Potassium Ion Efflux in Infected Macrophages[▽]

Takeshi Kurenuma,[1] Ikuo Kawamura,[1]* Hideki Hara,[1] Ryosuke Uchiyama,[2] Sylvia Daim,[1] Sita Ramyamali Dewamitta,[1] Shunsuke Sakai,[1] Kohsuke Tsuchiya,[1] Takamasa Nomura,[1] and Masao Mitsuyama[1]

Department of Microbiology, Kyoto University Graduate School of Medicine, Kyoto 606-8501, Japan,[1] and Department of Microbiology, Hyogo College of Medicine, Nishinomiya 663-8501, Japan[2]

Received 6 January 2009/Returned for modification 25 March 2009/Accepted 2 July 2009

A genomic locus called "region of difference 1" (RD1) in *Mycobacterium tuberculosis* has been shown to contribute to the generation of host protective immunity as well as to the virulence of the bacterium. To gain insight into the molecular mechanism, we investigated the difference in the cytokine-inducing ability between H37Rv and a mutant strain deficient for RD1 (ΔRD1). We found that RD1 is implicated in the production of caspase-1-dependent cytokines, interleukin-18 (IL-18) and IL-1β, from infected macrophages. The expression of these cytokines was similarly induced after infection with H37Rv and ΔRD1. However, the activation of caspase-1 was observed only in H37Rv-infected macrophages. The cytokine production and caspase-1 activation were induced independently of type I interferon receptor signaling events. We also found that the activation of caspase-1 was markedly inhibited with increasing concentrations of extracellular KCl. Furthermore, the production of IL-18 and IL-1β and caspase-1 activation were induced independently of a P2X7 purinergic receptor, and the inability of ΔRD1 in caspase-1 activation was compensated for by nigericin, an agent inducing the potassium ion efflux. Based on these results, we concluded that RD1 participates in caspase-1-dependent cytokine production via induction of the potassium ion efflux in infected macrophages.

Mycobacterium tuberculosis, an etiologic agent of human tuberculosis, is one of the leading threats to humans. It has been reported that *M. tuberculosis* still causes 9.2 million new cases of tuberculosis worldwide and 1.7 million deaths annually (49). The recent emergence of multidrug-resistant and extensively drug-resistant *M. tuberculosis* strains highlights the urgent need for extensive research unraveling the complex mechanism enabling the bacterium to be successfully parasitic in humans.

The protective immunity against *M. tuberculosis* is mediated mainly by Th1-type $CD4^+$ T cells and $CD8^+$ T cells. These T cells produce a large amount of cytokines, including gamma interferon (IFN-γ) and tumor necrosis factor alpha (TNF-α), resulting in the enhancement of macrophage bactericidal activity and the development of granulomas in which *M. tuberculosis* is killed and prevented from disseminating to the bloodstream and other tissues (12, 47). It has been demonstrated that T cells differentiate into Th1 cells in cooperation with several proinflammatory cytokines, such as interleukin-12 (IL-12), IL-18, and IFN-γ, that are produced by infiltrating dendritic cells, macrophages, and NK cells. A number of in vitro studies have shown that these cytokines are produced via recognition of pathogen-associated molecular patterns of *M. tuberculosis* by Toll-like receptors (TLRs) (43). However, the role of TLR-mediated signaling pathways in the protective immunity against *M. tuberculosis* is controversial. Abel et al. have shown that TLR4-deficient mice display reduced bacterial clearance during a long-term infection and develop chronic pneumonia (2). Drennan et al. have also reported that TLR2-deficient mice initially control an aerosol infection with *M. tuberculosis*, but develop increased bacterial burden and succumb to chronic pneumonia (8). On the other hand, recent studies have shown that TLRs are dispensable in the development of T-cell-mediated adaptive immunity, while myeloid differentiation protein 88 (MyD88) is required for restriction of the intracellular growth of *M. tuberculosis* (44). In addition, Fremond et al. (16) and Hölscher et al. (24) have shown that mice deficient for IL-1 receptor (IL-1R) succumbed to acute *M. tuberculosis* infection in a manner similar to mice deficient for MyD88, whereas mice deficient for TLR2, TLR4, TLR9, or Toll-IL-1R domain-containing adaptor protein could control acute *M. tuberculosis* infection to the same extent as wild-type mice. These findings suggest that MyD88 plays a much more prominent role in adaptive immunity than functioning as an adaptor molecule of TLRs, and the role of the MyD88-dependent IL-1R signaling pathway is necessary for induction of efficient protection against *M. tuberculosis*.

A genomic locus of *M. tuberculosis* called "region of difference 1" (RD1) was first discovered as a locus that is absent in a genome of *Mycobacterium bovis* BCG (30). RD1 is 9.5 kb in length and comprises nine genes, including the genes that encode the secretory proteins ESAT-6 (6-kDa early secreted antigen target) and CFP-10 (10-kDa culture filtrate protein). The other genes encode components of a secretion system that is called ESX-1 (ESAT-6 system 1). It is supposed that more than 14 proteins contribute to this secretion system (1). Al-

* Corresponding author. Mailing address: Department of Microbiology, Kyoto University Graduate School of Medicine, Yoshidakonoecho, Sakyo-ku, Kyoto 606-8501, Japan. Phone: 81-75-753-4447. Fax: 81-75-753-4446. E-mail: ikuo_kawamura@mb.med.kyoto-u.ac.jp.

▽ Published ahead of print on 13 July 2009.